A Communication-Efficient Distributed Gradient Clipping Algorithm for Training Deep Neural Networks

Mingrui Liu[1]*, **Zhenxun Zhuang**[2], **Yunwen Lei**[3], **Chunyang Liao**[4]
[1]Department of Computer Science, George Mason University, Fairfax, VA 22030, USA
[2]Meta Platforms, Inc., Bellevue, WA, 98004, USA
[3] School of Computer Science, University of Birmingham, United Kingdom
[4] Department of Mathematics, Texas A&M University, College Station, Texas 77840, USA
mingruil@gmu.edu, oldboymls@gmail.com, yunwen.lei@hotmail.com

Abstract

In distributed training of deep neural networks, people usually run Stochastic Gradient Descent (SGD) or its variants on each machine and communicate with other machines periodically. However, SGD might converge slowly in training some deep neural networks (e.g., RNN, LSTM) because of the exploding gradient issue. Gradient clipping is usually employed to address this issue in the single machine setting, but exploring this technique in the distributed setting is still in its infancy: it remains mysterious whether the gradient clipping scheme can take advantage of multiple machines to enjoy parallel speedup. The main technical difficulty lies in dealing with nonconvex loss function, non-Lipschitz continuous gradient, and skipping communication rounds simultaneously. In this paper, we explore a relaxed-smoothness assumption of the loss landscape which LSTM was shown to satisfy in previous works, and design a communication-efficient gradient clipping algorithm. This algorithm can be run on multiple machines, where each machine employs a gradient clipping scheme and communicate with other machines after multiple steps of gradient-based updates. Our algorithm is proved to have $O\left(\frac{1}{N\epsilon^4}\right)$ iteration complexity and $O(\frac{1}{\epsilon^3})$ communication complexity for finding an ϵ-stationary point in the homogeneous data setting, where N is the number of machines. This indicates that our algorithm enjoys linear speedup and reduced communication rounds. Our proof relies on novel analysis techniques of estimating truncated random variables, which we believe are of independent interest. Our experiments on several benchmark datasets and various scenarios demonstrate that our algorithm indeed exhibits fast convergence speed in practice and thus validates our theory.

1 Introduction

Deep learning has achieved tremendous successes in many domains including computer vision [23, 15], natural language processing [5] and game [39]. To obtain good empirical performance, people usually need to train large models on a huge amount of data, and it is usually very computationally expensive. To speed up the training process, distributed training becomes indispensable [4]. For example, Goyal et al. [12] trained a ResNet-50 on ImageNet dataset by distributed SGD with minibatch size 8192 on 256 GPUs in only one hour, which not only matches the small minibatch

*Corresponding Author. The code is available at https://github.com/MingruiLiu-ML-Lab/Communication-Efficient-Local-Gradient-Clipping

36th Conference on Neural Information Processing Systems (NeurIPS 2022).

Table 1: Comparison of Iteration and Communication Complexity of Different Algorithms for finding a point whose gradient's magnitude is smaller than ϵ (i.e., ϵ-stationary point defined in Definition 3), N is the number of machines, the meaning of other constants can be found in Assumption 1. For the complexity of [9] in this table, we assume the gradient norm is upper bounded by M such that the gradient is $(L_0 + L_1 M)$-Lipschitz. However, the original paper of [9] does not require bounded gradient; instead, they require L-Lipschitz gradient and bounded variance σ^2. Under their assumption, their complexity result is $O\left(\Delta L\epsilon^{-2} + \Delta L\sigma^2\epsilon^{-4}\right)$.

Algorithm	Setting	Iteration Complexity	Communication Complexity
SGD [9]	Single	$O\left(\Delta(L_0 + L_1 M)\epsilon^{-2} + \Delta(L_0 + L_1 M)\sigma^2\epsilon^{-4}\right)$	N/A
Clipped SGD [51]	Single	$O\left((\Delta + (L_0 + L_1\sigma)\sigma^2 + \sigma L_0^2/L_1)^2)\epsilon^{-4}\right)$	N/A
Clipping Framework [50]	Single	$O\left(\Delta L_0\sigma^2\epsilon^{-4}\right)$	N/A
Naive Parallel of [50]	Distributed	$O\left(\Delta L_0\sigma^2/(N\epsilon^4)\right)$	$O\left(\Delta L_0\sigma^2/(N\epsilon^4)\right)$
Ours (this work)	Distributed	$O(\Delta L_0\sigma^2/(N\epsilon^4))$	$O\left(\Delta L_0\sigma\epsilon^{-3}\right)$

accuracy but also enjoys parallel speedup, and hence improves the running time. Recently, local SGD [40, 47], as a variant of distributed SGD, achieved tremendous attention in federated learning community [29]. The local SGD algorithm runs multiple steps of SGD on each machine before communicating with other clients.

Despite the empirical success of distributed SGD and its variants (e.g., local SGD) in deep learning, they may not exhibit good performance when training some neural networks (e.g., Recurrent Neural Networks, LSTMs), due to the exploding gradient problem [33, 34]. To address this issue, Pascanu et al. [34] proposed to use the gradient clipping strategy, and it has become a standard technique when training language models [8, 35, 31]. There are some recent works trying to theoretically explain gradient clipping from the perspective of non-convex optimization [51, 50]. These works are built upon an important observation made in [51]: for certain neural networks such as LSTM, the gradient does not vary uniformly over the loss landscape (i.e., the gradient is not Lipschitz continuous with a uniform constant), and the gradient Lipschitz constant can scale linearly with respect to the gradient norm. This is referred to as the relaxed smoothness condition (i.e., (L_0, L_1)-smoothness defined in Definition 2), which generalizes but strictly relaxes the usual smoothness condition (i.e., L-smoothness defined in Definition 1). Under the relaxed smoothness condition, Zhang et al. [51, 50] proved that gradient clipping enjoys polynomial-time iteration complexity for finding the first-order stationary point in the single machine setting, and it can be arbitrarily faster than fix-step gradient descent. In practice, both distributed learning and gradient clipping are important techniques to accelerate neural network training. However, the theoretical analysis of gradient clipping is only restricted to the single machine setting [51, 50]. Hence it naturally motivates us to consider the following question:

Is it possible that the gradient clipping scheme can take advantage of multiple machines to enjoy parallel speedup in training deep neural networks, with only infrequent communication?

In this paper, we give an affirmative answer to the above question. Built upon the relaxed smoothness condition as in [51, 50], we design a communication-efficient distributed gradient clipping algorithm. The key characteristics of our algorithm are: (i) unlike naive parallel gradient clipping algorithm [2] which requires averaging model weights and gradients from all machines for every iteration, our algorithm only aggregates weights with other machines after a certain number of local updates on each machine; (ii) our algorithm clips the gradient according to the norm of the local gradient on each machine, instead of the norm of the averaged gradients across machines as in the naive parallel algorithm. These key features make our algorithm amenable to the distributed setting with infrequent communication, and it is nontrivial to establish desired theoretical guarantees (e.g., linear speedup, reduced communication complexity). The main difficulty in the analysis lies in dealing with the nonconvex objective function, non-Lipschitz continuous gradient, and skipping communication rounds simultaneously. Our main contribution is summarized as the following:

[2] Naive Parallel of [50] stands for the algorithm which clips the gradient based on the globally averaged gradient at every iteration with constant minibatch size.

- We design a novel communication-efficient distributed stochastic local gradient clipping algorithm, namely CELGC, for solving a nonconvex optimization problem under the relaxed smoothness condition. The algorithm only needs to clip the gradient according to the local gradient's magnitude and globally averages the weights on all machines periodically. To the best of our knowledge, this is the first work proposing communication-efficient distributed stochastic gradient clipping algorithms under the relaxed smoothness condition.
- Under the relaxed smoothness condition, we prove iteration and communication complexity results of our algorithm for finding an ϵ-stationary point, when each machine has access to the same data distribution. First, comparing with [50], we prove that our algorithm enjoys linear speedup, which means that the iteration complexity of our algorithm is reduced by a factor of N (the number of machines). Second, comparing with the naive parallel version of the algorithm of [50], we prove that our algorithm enjoys better communication complexity. The detailed comparison over existing algorithms under the same relaxed smoothness condition is described in Table 1. To achieve this result, we introduce a novel technique of estimating truncated random variables, which is of independent interest and could be applied in related problems involving truncation operations such as gradient clipping.
- We empirically verify our theoretical results by conducting experiments on different neural network architectures on benchmark datasets. The experimental results demonstrate that our proposed algorithm indeed exhibits speedup in practice.

2 Related Work

Gradient Clipping/Normalization Algorithms In deep learning literature, gradient clipping (normalization) technique was initially proposed by [34] to address the issue of exploding gradient problem in [33], and it has become a standard technique when training language models [8, 35, 31].It is shown that gradient clipping is robust and can mitigate label noise [30]. Recently gradient normalization techniques [45, 46] were applied to train deep neural networks on the very large batch setting. For example, You et al. [45] designed the LARS algorithm to train a ResNet50 on ImageNet with batch size 32k, which utilized different learning rates according to the norm of the weights and the norm of the gradient. In optimization literature, gradient clipping (normalization) was used in early days in the field of convex optimization [7, 1, 38]. Nesterov [32] and Hazan et al. [14] considered normalized gradient descent for quasi-convex functions in deterministic and stochastic cases respectively. Gorbunov et al. [10] designed an accelerated gradient clipping method to solve convex optimization problems with heavy-tailed noise in stochastic gradients. Mai and Johansson [26] established the stability and convergence of stochastic gradient clipping algorithms for convex and weakly convex functions. In nonconvex optimization, Levy [24] showed that normalized gradient descent can escape from saddle points. Cutosky and Mehta [3] showed that adding a momentum provably improves the normalized SGD in nonconvex optimization. Zhang et al. [51] and Zhang et al. [50] analyzed the gradient clipping for nonconvex optimization under the relaxed smoothness condition rather than the traditional L-smoothness condition in nonconvex optimization [9]. However, all of them only consider the algorithm in the single machine setting or the naive parallel setting, and none of them can apply to the distributed setting where only limited communication is allowed.

Communication-Efficient Algorithms in Distributed and Federated Learning In large-scale machine learning, people usually train their model using first-order methods on multiple machines and these machines communicate and aggregate their model parameters periodically. When the function is convex, there is a scheme named one-shot averaging [56, 28, 54, 37], in which every machine runs a stochastic approximation algorithm and averages the model weights across machines only at the very last iteration. The one-shot averaging scheme is communication-efficient and enjoys statistical convergence with one pass of the data [54, 37, 16, 22], but the training error may not converge in practice. Mcmahan et al. [29] considered the Federated Learning setting where the data is decentralized and might be non-i.i.d. across devices and communication is expensive and designed the very first algorithm for federated learning (a.k.a., FedAvg). Stich [40] considered a concrete case of FedAvg, namely local SGD, which runs SGD independently in parallel on different works and averages the model parameters only once in a while. Stich [40] also showed that local SGD enjoys linear speedup for strongly-convex objective functions. There are also some works analyzing local SGD and its variants on convex [6, 20, 19, 43, 44, 11, 49] and nonconvex smooth functions [55, 47, 48, 17, 41, 25, 2, 13, 19]. Recently, Woodworth et al. [43, 44] analyzed advantages

and drawbacks of local SGD compared with minibatch SGD for convex objectives. Woodworth et al. [42] proved hardness results for distributed stochastic convex optimization. Reddi et al. [36] introduced a general framework of federated optimization and designed several federated versions of adaptive optimizers. Zhang et al. [52] considered employing gradient clipping to optimize L-smooth functions and achieve differential privacy. Koloskova et al. [21] developed a unified theory of decentralized SGD with changing topology and local updates for smooth functions. Zhang et al. [53] developed a federated learning framework for nonconvex smooth functions for non-i.i.d. data. Due to a vast amount of literature on federated learning and limited space, we refer readers to [18] and references therein. However, all of these works either assume the objective function is convex or L-smooth. To the best of our knowledge, our algorithm is the first communication-efficient algorithm that does not rely on these assumptions but still enjoys linear speedup.

3 Preliminaries, Notations and Problem Setup

Preliminaries and Notations Denote $\|\cdot\|$ by the Euclidean norm. We denote $f : \mathbb{R}^d \to \mathbb{R}$ as the overall loss function, and $F : \mathbb{R}^d \to \mathbb{R}$ as the loss function on i-th machine, where $i \in [N] := \{1, \ldots, N\}$. Denote $\nabla h(\mathbf{x})$ as the gradient of h evaluated at the point $\mathbf{x}$, and denote $\nabla h(\mathbf{x}; \xi)$ as the stochastic gradient of h calculated based on sample ξ.

Definition 1 (L-smoothness)**.** *A function h is L-smooth if $\|\nabla h(\mathbf{x}) - \nabla h(\mathbf{y})\| \leq L\|\mathbf{x} - \mathbf{y}\|$ for all $\mathbf{x}, \mathbf{y} \in \mathbb{R}^d$.*

Definition 2 ((L_0, L_1)-smoothness)**.** *A second order differentiable function h is (L_0, L_1)-smooth if $\|\nabla^2 h(\mathbf{x})\| \leq L_0 + L_1\|\nabla h(\mathbf{x})\|$ for any $\mathbf{x} \in \mathbb{R}^d$.*

Definition 3 (ϵ-stationary point)**.** *$\mathbf{x} \in \mathbb{R}^d$ is an ϵ-stationary point of the function h if $\|\nabla h(\mathbf{x})\| \leq \epsilon$.*

Remark: (L_0, L_1)-smoothness is strictly weaker than L-smoothness. First, we know that L-smooth functions is (L_0, L_1)-smooth with $L_0 = L$ and $L_1 = 0$. However the reverse is not true. For example, consider the function $h(x) = x^4$, we know that the gradient is not Lipschitz continuous and hence h is not L-smooth, but $|h''(x)| = 12x^2 \leq 12 + 3 \times 4|x|^3 = 12 + 3|h'(x)|$, so $h(x) = x^4$ is $(12, 3)$-smooth. Zhang et al. [51] empirically showed that the (L_0, L_1)-smoothness holds for the AWD-LSTM [31]. In nonconvex optimization literature [9, 50], the goal is to find an ϵ-stationary point since it is NP-hard to find a global optimal solution for a general nonconvex function.

Problem Setup In this paper, we consider the following optimization problem using N machines:

$$\min_{\mathbf{x} \in \mathbb{R}^d} f(\mathbf{x}) = \mathbb{E}_{\xi \sim \mathcal{D}} \left[F(\mathbf{x}; \xi) \right], \tag{1}$$

where $\mathcal{D}$ stands for the data distribution which each machine has access to, and f is the population loss function.

We make the following assumptions throughout the paper.

Assumption 1. *(i) $f(\mathbf{x})$ is (L_0, L_1)-smooth, i.e., $\|\nabla^2 f(\mathbf{x})\| \leq L_0 + L_1\|\nabla f(\mathbf{x})\|$, for $\forall \mathbf{x} \in \mathbb{R}^d$.*

(ii) There exists $\Delta > 0$ such that $f(\mathbf{x}_0) - f_* \leq \Delta$, where f_* is the global optimal value of f.

(iii) For all $\mathbf{x} \in \mathbb{R}^d$, $\mathbb{E}_{\xi \sim \mathcal{D}} \left[\nabla F(\mathbf{x}; \xi) \right] = \nabla f(\mathbf{x})$, and $\|\nabla F(\mathbf{x}; \xi) - \nabla f(\mathbf{x})\| \leq \sigma$ almost surely.

(iv) The distribution of $\nabla F(\mathbf{x}; \xi)$ is symmetric around its mean $\nabla f(\mathbf{x})$, and the density is monotonically decreasing over the ℓ_2 distance between the mean and the value of random variable.

Remark: The Assumption 1 (i) means that the loss function satisfies the relaxed-smoothness condition, and it holds when training a language model with LSTMs. We consider the homogeneous distributed learning setting, where each machine has access to same data distribution as in [44]. Assumption 1 (ii) and (iii) are standard assumptions in nonconvex optimization [9, 51]. Note that it is usually assumed that the stochastic gradient is unbiased and has bounded variance [9], but in the relaxed smoothness setting, we follow [51] to assume we have unbiased stochastic gradient with almost surely bounded deviation σ. Assumption 1 (iv) assumes the noise is unimodal and symmetric around its mean, which we empirically verify in Appendix E. Examples satisfying (iii) and (iv) include truncated Gaussian distribution, truncated student's t-distribution, etc.

Algorithm 1 Communication Efficient Local Gradient Clipping (CELGC)

for $t = 0, \ldots, T$ **do**
  Each node i samples its stochastic gradient $\nabla F(\mathbf{x}_t^i; \xi_t^i)$, where $\xi_t^i \sim \mathcal{D}$.
  Each node i updates it local solution **in parallel**:

$$\mathbf{x}_{t+1}^i = \mathbf{x}_t^i - \min\left(\eta, \frac{\gamma}{\|\nabla F(\mathbf{x}_t^i; \xi_t^i)\|}\right) \nabla F(\mathbf{x}_t^i; \xi_t^i) \tag{2}$$

  if t is a multiple of I **then**
    Each worker resets the local solution as the averaged solution across nodes:

$$\mathbf{x}_t^i = \widehat{\mathbf{x}} := \frac{1}{N} \sum_{j=1}^{N} \mathbf{x}_t^j \qquad \forall i \in \{1, \ldots, N\} \tag{3}$$

  end if
end for

4 Algorithm and Theoretical Analysis

4.1 Main Difficulty and the Algorithm Design

We briefly present the main difficulty in extending the single machine setting [50] to the distributed setting. In [50], they split the contribution of decreasing objective value by considering two cases: clipping large gradients and keeping small gradients. If communication is allowed at every iteration, then we can aggregate gradients on each machine and determine whether we should clip or keep the averaged gradient or not. However, in our setting, communicating with other machines at every iteration is not allowed. This would lead to the following difficulties: (i) the averaged gradient may not be available to the algorithm if communication is limited, so it is hard to determine whether clipping operation should be performed or not; (ii) the model weight on every machine may not be the same when communication does not happen at the current iteration; (iii) the loss function is not L-smooth, so the usual local SGD analysis for L-smooth functions cannot be applied in this case.

To address this issue, we design a new algorithm, namely Communication-Efficient Local Gradient Clipping (CELGC), which is presented in Algorithm 1. The algorithm calculates a stochastic gradient and then performs multiple local gradient clipping steps on each machine in parallel, and aggregates model parameters on all machines after every I steps of local updates. We aim to establish iteration and communication complexity for Algorithm 1 for finding an ϵ-stationary point when $I > 1$.

4.2 A Lemma for Truncated Random Variables

As indicated in the previous subsection, Algorithm 1 clips gradient on each local machine. This feature greatly complicates the analysis: it is difficult to get an unbiased estimate of the stochastic gradient when its magnitude is not so large such that clipping does not happen. The reason is due to the dependency between random variables (i.e., stochastic gradient and the indicator of clipping). To get around of this difficulty, we introduce the following Lemma for estimating truncated random variables.

Lemma 1. *Denote by* $\mathbf{g} \in \mathbb{R}^d$ *a random vector. Suppose the distribution of* $\mathbf{g}$ *is symmetric around its mean, and the density is monotonically decreasing over the* ℓ_2 *distance between the mean and the value of random variable, then there exists* $\Lambda = diag(c_1, \ldots, c_d)$ *and* $0 < c_i \leq 1$ *with* $i = 1, \ldots, d$ *such that*

$$\mathbb{E}\left[\mathbf{g}\mathbb{I}(\|\mathbf{g}\| \leq \alpha)\right] = Pr(\|\mathbf{g}\| \leq \alpha)\Lambda\mathbb{E}\left[\mathbf{g}\right], \tag{4}$$

where $\alpha > 0$ *is a constant,* $\mathbb{I}(\cdot)$ *is the indicator function.*

The proof of Lemma 1 is included in Appendix B. This Lemma provides an unbiased estimate for a truncated random variable. In the subsequent of this paper, we regard $\mathbf{g}$ in the Lemma as the stochastic gradient and α as the clipping threshold. In addition, we define $c_{\min} = \min(c_1, \ldots, c_d)$, and $c_{\max} = \max(c_1, \ldots, c_d)$. We have $0 < c_{\min} \leq c_{\max} \leq 1$.

4.3 Main Results

Theorem 1. *Suppose Assumption 1 holds and $\sigma \geq 1$. Take $\epsilon \leq \min(\frac{AL_0}{BL_1}, 0.1)$ be a small enough constant and $N \leq \min(\frac{1}{\epsilon}, \frac{14AL_0}{5BL_1\epsilon})$. In Algorithm 1, choose $I \leq \sqrt{\frac{1}{c_{\min}}}\frac{\sigma}{N\epsilon}$, $\gamma \leq c_{\min}\frac{N\epsilon}{28\sigma}\min\{\frac{\epsilon}{AL_0}, \frac{1}{BL_1}\}$ and the fixed ratio $\frac{\gamma}{\eta} = 5\sigma$, where $A \geq 1$ and $B \geq 1$ are constants which will be specified in the proof, and run Algorithm 1 for $T = O\left(\frac{\Delta L_0 \sigma^2}{N\epsilon^4}\right)$ iterations. Define $\bar{\mathbf{x}}_t = \frac{1}{N}\sum_{i=1}^N \mathbf{x}_t^i$. Then we have $\frac{1}{T}\sum_{t=1}^T \mathbb{E}\|\nabla f(\bar{\mathbf{x}}_t)\| \leq 9\epsilon$.*

Remark: We have some implications of Theorem 1. When the number of machines is not large (i.e., $N \leq O(1/\epsilon)$) and the number of skipped communications is not large (i.e., $I \leq O(\sigma/\epsilon N)$), then with proper setting of the learning rate, we have following observations. First, our algorithm enjoys linear speedup, since the number of iterations we need to find an ϵ-stationary point is divided by the number of machines N when comparing the single machine algorithm in [50]. Second, our algorithm is communication-efficient, since the communication complexity (a.k.a., number of rounds) is $T/I = O\left(\Delta L_0 \sigma \epsilon^{-3}\right)$, which provably improves the naive parallel gradient clipping algorithm of [50] with $O(\Delta L_0 \sigma^2/(N\epsilon^4))$ communication complexity when $N \leq O(1/\epsilon)$.

Another important fact is that both iteration complexity and communication complexity only depend on L_0 while being independent of L_1 and the gradient upper bound M. This indicates that our algorithm does not suffer from slow convergence even if these quantities are large. This is in line with [50] as well. In addition, local gradient clipping is a good mechanism to alleviate the bad effects brought by a rapidly changing loss landscape (e.g., some language models such as LSTM).

4.4 Sketch of the Proof of Theorem 1

In this section, we present the sketch of our proof of Theorem 1. The detailed proof can be found in Appendix C. The key idea in our proof is to establish the descent property of the sequence $\{f(\bar{\mathbf{x}}_t)\}_{t=0}^T$ in the distributed setting under the relaxed smoothness condition, where $\bar{\mathbf{x}}_t = \frac{1}{N}\sum_{i=1}^t \mathbf{x}_t^i$ is the averaged weight across all machines at t-th iteration. The main challenge is that the descent property of (L_0, L_1)-smooth function in the distributed setting does not naturally hold, which is in sharp contrast to the usual local SGD proof for L-smooth functions. To address this challenge, we need to carefully study whether the algorithm is able to decrease the objective function in different situations. Our main technical innovations in the proof are listed as the following.

First, we monitor the algorithm's progress in decreasing the objective value according to some novel measures. The measures we use are the magnitude of the gradient evaluated at the averaged weight and the magnitude of local gradients evaluated at the individual weights on every machine. To this end, we introduce Lemma 3, whose goal is to carefully inspect how much progress the algorithm makes, according to the magnitude of local gradients calculated on each machine. The reason is that the local gradient's magnitude is an indicator of whether the clipping operation happens or not. For each fixed iteration t, we define $J(t) = \{i \in [N] : \|\nabla F(\mathbf{x}_t^i, \xi_t^i)\| \geq \gamma/\eta\}$ and $\bar{J}(t) = [N] \setminus J(t)$. Briefly speaking, $J(t)$ contains all machines that perform clipping operation at iteration t and $\bar{J}(t)$ is the set of machines that do not perform clip operation at iteration t. In Lemma 3, we perform the one-step analysis and consider all machines with different clipping behaviors at the iteration t. The proof of Lemma 3 crucially relies on the lemma for estimating truncated random variables (i.e., Lemma 1) to calculate the expectation of non-clipped gradients.

Second, Zhang et al. [50] inspect their algorithm's progress by considering the magnitude of the gradient at different iterations, so they treat every iteration differently. However, this approach does not work in the distributed setting with infrequent communication since one cannot get access to the averaged gradient across machines at every iteration. Instead, we treat every iteration of the algorithm as the same but consider the progress made by each machine.

Third, by properly choosing hyperparameters (η, γ, I) and using an amortized analysis, we prove that our algorithm can decrease the objective value by a sufficient amount, and the sufficient decrease is mainly due to the case where the gradient is not too large (i.e., clipping operations do not happen). This important insight allows us to better characterize the training dynamics.

Now we present how to proceed with the proof in detail.

Lemma 2 characterizes the ℓ_2 error between averaged weight and individual weights at t-th iteration.

Lemma 2. *Under Assumption 1, for any i and t, Algorithm 1 ensures $\|\bar{\mathbf{x}}_t - \mathbf{x}_t^i\| \leq 2\gamma I$ holds almost surely.*

Lemma 5 and Lemma 6 (in Appendix A) are properties of (L_0, L_1)-smooth functions we need to use. To make sure they work, we need $2\gamma I \leq c/L_1$ for some $c > 0$. This is proved in the proof of Theorem 1 (in Appendix C).

Let $J(t)$ be the index set of i such that $\|\nabla F(\mathbf{x}_t^i, \xi_t^i)\| \geq \frac{\gamma}{\eta}$ at fixed iteration t, i.e., $J(t) = \{i \in [N] \mid \|\nabla F(\mathbf{x}_t^i; \xi_t^i)\| \geq \gamma/\eta\}$. Lemma 3 characterizes how much progress we can get in one iteration of Algorithm 1, which is decomposed into contributions from every machine (note that $J(t) \cup \bar{J}(t) = \{1, \ldots, N\}$ for every t).

Lemma 3. *Let $J(t)$ be the set defined as above. If $2\gamma I \leq c/L_1$ for some $c > 0$, $AL_0\eta \leq 1/2$, and $\gamma/\eta = 5\sigma$, then we have*

$$
\begin{aligned}
&\mathbb{E}[f(\bar{\mathbf{x}}_{t+1}) - f(\bar{\mathbf{x}}_t)] \\
\leq &\frac{1}{N}\mathbb{E}\sum_{i\in J(t)}\left[-\frac{2\gamma}{5}\|\nabla f(\bar{\mathbf{x}}_t)\| - \frac{3\gamma^2}{5\eta} + \frac{50AL_0\eta^2\sigma^2}{N} + \frac{7\gamma}{5}\|\nabla F(\mathbf{x}_t^i;\xi_t^i) - \nabla f(\bar{\mathbf{x}}_t)\| + AL_0\gamma^2 + \frac{BL_1\gamma^2\|\nabla f(\bar{\mathbf{x}}_t)\|}{2}\right] \\
+&\mathbb{E}\frac{1}{N}\sum_{i\in \bar{J}(t)}\left[-\frac{\eta c_{\min}}{2}\|\nabla f(\bar{\mathbf{x}}_t)\|^2 + 4\gamma^2 I^2 A^2 L_0^2\eta + 4\gamma^2 I^2 B^2 L_1^2\eta\|\nabla f(\bar{\mathbf{x}}_t)\|^2 + \frac{50AL_0\eta^2\sigma^2}{N} + \frac{BL_1\gamma^2\|\nabla f(\bar{\mathbf{x}}_t)\|}{2}\right],
\end{aligned}
$$

where $A = 1 + e^c - \frac{e^c-1}{c}$ and $B = \frac{e^c-1}{c}$.

Lemma 4 quantifies an upper bound of the averaged ℓ_2 error between the local gradient evaluated at the local weight and the gradient evaluated at the averaged weight.

Lemma 4. *Suppose Assumption 1 holds. When $2\gamma I \leq c/L_1$ for some $c > 0$, the following inequality holds for every i almost surely with $A = 1 + e^c - \frac{e^c-1}{c}$ and $B = \frac{e^c-1}{c}$:*

$$
\left\|\nabla F(\mathbf{x}_t^i;\xi_t^i) - \nabla f(\bar{\mathbf{x}}_t)\right\| \leq \sigma + 2\gamma I(AL_0 + BL_1\|\nabla f(\bar{\mathbf{x}}_t)\|).
$$

Putting all together Suppose our algorithm runs T iterations. Taking summation on both sides of Lemma 3 over all $t = 0, \ldots, T-1$, we are able to get an upper bound of $\sum_{t=0}^{T-1}\mathbb{E}\left[f(\bar{\mathbf{x}}_{t+1}) - f(\bar{\mathbf{x}}_t)\right] = \mathbb{E}\left[f(\bar{\mathbf{x}}_T) - f(\bar{\mathbf{x}}_0)\right]$. Note that $\mathbb{E}\left[f(\bar{\mathbf{x}}_T) - f(\bar{\mathbf{x}}_0)\right] \geq -\Delta$ due to Assumption 1, so we are able to get an upper bound of gradient norm. For details, please refer to the proof of Theorem 1 in Appendix C.

5 Experiments

We conduct extensive experiments to validate the merits of our algorithm on various tasks (e.g., image classification, language modeling). In the main text below, we consider the homogeneous data setting where each machine has the same data distribution and every machine participate the communication at each round. In the Appendix D, we also test our algorithm in the general federated learning setting (e.g., partial participation of machines), ablation study on small/large batch-sizes, and other experiments, etc.

We conduct each experiment in two nodes with 4 Nvidia-V100 GPUs on each node. In our experiments, one "machine" corresponds to one GPU, and we use the word "GPU" and "machine" in this section interchangeably. We compared our algorithm with the baseline across three deep learning benchmarks: CIFAR-10 image classification with ResNet, Penn Treebank language modeling with LSTM, and Wikitext-2 language modeling with LSTM, and ImageNet classification with ResNet. All algorithms and the training framework are implemented in Pytorch 1.4. Due to limited computational resources, for our algorithms, we choose same hyperparameters like the clipping thresholds according to the best-tuned baselines unless otherwise specified.

We compare our algorithm of different I with the baseline, which is the naive parallel version of the algorithm in [50]. We want to re-emphasize that the difference is that the baseline algorithm needs to average the model weights and local gradients at every iteration while ours only requires averaging the model weights after every I iterations. We find that our algorithm with a range of values of I can

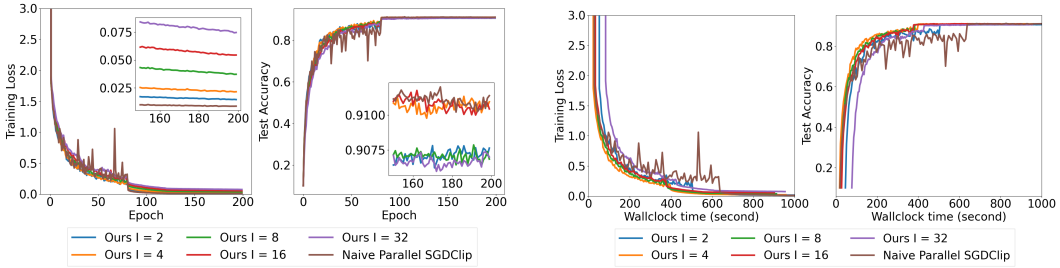

(a) Over epoch

(b) Over wall clock time

Figure 1: Algorithm 1 with different I: Training loss and test accuracy v.s. (Left) epoch and (right) wall clock time on training a 56 layer Resnet to do image classification on CIFAR10.

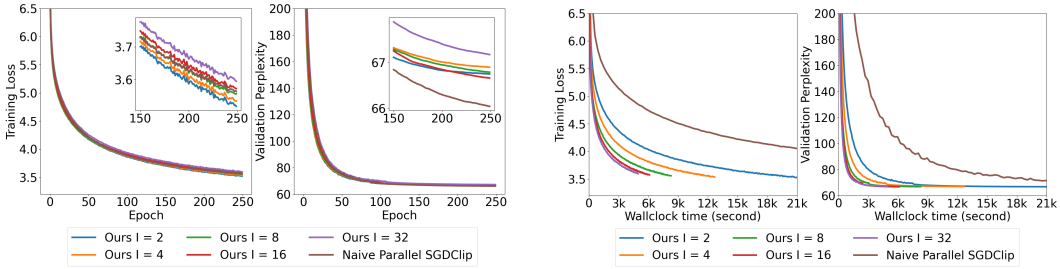

(a) Over epoch

(b) Over Wall clock time

Figure 2: Algorithm 1 with different I: Training loss and validation perplexity v.s. (Left) epoch and (right) wall clock time on training an AWD-LSTM to do language modeling on Penn Treebank.

match the results of the baseline in terms of epochs on different models and data. This immediately suggests that our algorithm will gain substantial speedup in terms of the wall clock time, which is also supported by our experiments.

5.1 Effects of Skipping Communication

We focus on one feature of our algorithm: skipping communication rounds. Theorem 1 says that our algorithm enjoys reduced communication complexity since every node only communicates with other nodes periodically with node synchronization interval length I. To study how communication skipping affects the convergence of Algorithm 1, we run it with $I \in \{2, 4, 8, 16, 32\}$.

CIFAR-10 classification with ResNet-56. We train the standard 56-layer ResNet [15] architecture on CIFAR-10. We use SGD with clipping as the baseline algorithm with a stagewise decaying learning rate schedule, following the widely adopted fashion on training the ResNet architecture. Specifically, we use the initial learning rate $\eta = 0.3$, the clipping threshold $\gamma = 1.0$, and decrease the learning rate by a factor of 10 at epoch 80 and 120. The local batch size at each GPU is 64. These parameter settings follow that of [47].

The results are illustrated in Figure 1. Figure 1a shows the convergence of training loss and test accuracy v.s. the number of epochs that are jointly accessed by all GPUs. This means that, if the x-axis value is 8, then each GPU runs 1 epoch of training data. The same convention applied to all other figures for multiple GPU training in this paper. Figure 1b verifies our algorithm's advantage of skipping communication by plotting the convergence of training loss and test accuracy v.s. the wall clock time. Overall, we can clearly see that our algorithm matches the baseline epoch-wise but greatly speeds up wall-clock-wise.

Language modeling with LSTM on Penn Treebank. We adopt the 3-layer AWD-LSTM [31] to do language modeling on Penn Treebank (PTB) dataset [27](word level). We use SGD with clipping as the baseline algorithm with the clipping threshold $\gamma = 7.5$. The local batch size at each GPU is 3. These parameter settings follow that of [50]. We fine-tuned the initial learning rate η for all algorithms (including the baseline) by choosing the one giving the smallest final training loss in the range $\{0.1, 0.5, 1, 5, 10, 20, 30, 40, 50, 100\}$.

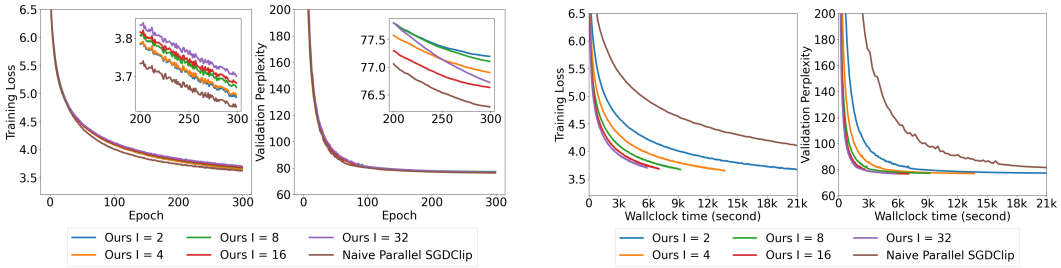

(a) Over epoch

(b) Over Wall clock time

Figure 3: Algorithm 1 with different I: Training loss and validation perplexity v.s. (Left) epoch and (right) wall clock time on training an AWD-LSTM to do language modeling on Wikitext-2.

We report the results in Figure 2. It can be seen that we can match the baseline in both training loss and validation perplexity epoch-wise while gaining substantial speedup (4x faster for $I = 4$) wall-clock-wise.

Language modeling with LSTM on Wikitext-2. We adopt the 3-layer AWD-LSTM [31] to do language modeling on Wikitext-2 dataset [27](word level). We use SGD with clipping as the baseline algorithm with the clipping threshold $\gamma = 7.5$. The local batch size at each GPU is 10. These parameter settings follow that of [31]. We fine-tuned the initial learning rate η for all algorithms (including the baseline) by choosing the one giving the smallest final training loss in the range $\{0.1, 0.5, 1, 5, 10, 20, 30, 40, 50, 100\}$.

We report the results in Figure 3. We can match the baseline in both training loss and validation perplexity epoch-wise, but we again obtain large speedup (4x faster for $I = 4$) wall-clock-wise. This, together with the above two experiments, clearly show our algorithm's effectiveness in speeding up the training in distributed settings. Another observation is that Algorithm 1 can allow relatively large I without hurting the convergence behavior.

ImageNet Classification with ResNet-50 We compared our algorithm with several baselines in training a ResNet-50 on ImageNet. We compared with two strong baselines: one is the Naive Parallel SGDClip, another is a well-accepted baseline for ImageNet by [12]. We run the experiments on 8 GPUs. We follow the settings of [12] to setup hyperparameter for baselines. Specifically, for every method, the initial learning rate is 0.0125, and we use the warmup with 5 epochs, batch size 32, momentum parameter 0.9, the weight decay 5×10^{-4}. The learning rate multiplying factor is 1 for the epoch $5 \sim 30$, and 0.1 for epoch $30 \sim 60$, 0.01 for epochs $60 \sim 80$, and 0.001 for epoch $80 \sim 90$. The clipping threshold for Naive Parallel SGDClip and our method CELGC are both set to be 1. We consider our algorithm with $I = 4$, i.e., our algorithm CELGC performs weight averaging after 4 steps of local stochastic gradient descent with gradient clipping on each GPU.

The results are shown in Figure 6. We report the performance of these methods from several different perspectives (training accuracy/validation accuracy versus epoch, and training accuracy/validation accuracy versus wallclock time). We can see that the training accuracy of our algorithm CELGC with $I = 4$ can match both baselines in terms of epoch (Figure 6a), but it is much better in terms of running time (Figure 6b).

5.2 Verifying Parallel Speedup

Figure 4 show the training loss and test accuracy v.s. the number of iterations. In the distributed setting, one iteration means running one step of Algorithm 1 on all machines; while in the single machine setting, one iteration means running one step of SGD with clipping. In our experiment, we use minibatch size 64 on every GPU in the distributed setting to run Algorithm 1, while we also use 64 minibatch size on the single GPU to run SGD with clipping. In the left two panels of Figure 4, we can clearly find that even with $I > 1$, our algorithm still enjoys parallel speedup, since our algorithm requires less number of iterations to converge to the same targets (e.g., training loss, test accuracy). This observation is consistent with our iteration complexity results in Theorem 1.

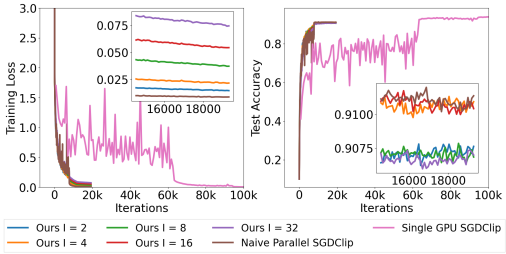

Figure 4: Performance v.s. # of iterations each GPU runs on training ResNet-56 on CIFAR-10 showing the parallel speedup.

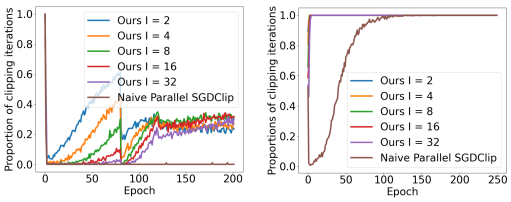

(a) CIFAR-10 (b) Penn Treebank

Figure 5: Proportions of iterations in each epoch in which clipping is triggered v.s. epochs showing clipping is very frequent.

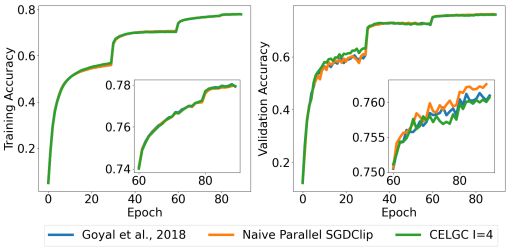

(a) Performance over epoch

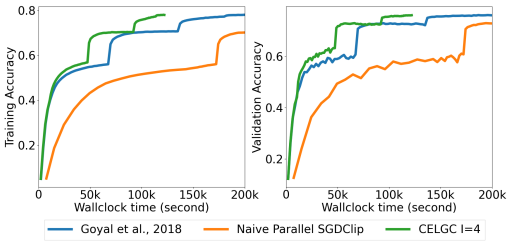

(b) Performance over wall clock time

Figure 6: Training loss and test accuracy v.s. epoch (left) and wall clock time (right) on training a Resnet-50 to do image classification on ImageNet.

5.3 Clipping Operation Happens Frequently

Figure 5 reports the proportion of iterations in each epoch that clipping is triggered. We observe that for our algorithm, clipping happens more frequently than the baseline, especially for NLP tasks. We conjecture that this is because we only used local gradients in each GPU to do the clipping without averaging them across all machines as the baseline did. This leads to more stochasticity of the norm of the gradient in our algorithm than the baseline, and thus causes more clippings to happen. This observation highlights the importance of studying clipping algorithms in the distributed setting. Another interesting observation is that clipping happens much more frequently when training language models than image classification models. Hence this algorithm is presumably more effective in training deep models in NLP tasks.

6 Conclusion

In this paper, we design a communication-efficient distributed stochastic local gradient clipping algorithm to train deep neural networks. By exploring the relaxed smoothness condition which was shown to be satisfied for certain neural networks, we theoretically prove both the linear speedup property and the improved communication complexity when the data distribution across machines is homogeneous. Our empirical studies show that our algorithm indeed enjoys parallel speedup and greatly improves the runtime performance in various federated learning scenarios (e.g., partial client participation). One limitation of our work is that our convergence analysis is only applicable for homogeneous data, and it would be interesting to analyze the settings of heterogeneous data theoretically in the future.

Acknowledgements

We would like to thank the anonymous reviewers for their help comments. Mingrui Liu is supported by a grant at George Mason University. Computations were run on ARGO, a research computing cluster provided by the Office of Research Computing at George Mason University (URL: https://orc.gmu.edu). The majority of work of Zhenxun Zhuang was done when he was a Ph.D. student at Boston University.

References

[1] Ya I Alber, Alfredo N. Iusem, and Mikhail V. Solodov. On the projected subgradient method for nonsmooth convex optimization in a hilbert space. *Mathematical Programming*, 81(1):23–35, 1998.

[2] Debraj Basu, Deepesh Data, Can Karakus, and Suhas Diggavi. Qsparse-local-sgd: Distributed sgd with quantization, sparsification and local computations. In *Advances in Neural Information Processing Systems*, pages 14668–14679, 2019.

[3] Ashok Cutkosky and Harsh Mehta. Momentum improves normalized sgd. In *International Conference on Machine Learning*, pages 2260–2268. PMLR, 2020.

[4] Jeffrey Dean, Greg Corrado, Rajat Monga, Kai Chen, Matthieu Devin, Mark Mao, Marc'aurelio Ranzato, Andrew Senior, Paul Tucker, Ke Yang, et al. Large scale distributed deep networks. In *Advances in neural information processing systems*, pages 1223–1231, 2012.

[5] Jacob Devlin, Ming-Wei Chang, Kenton Lee, and Kristina Toutanova. Bert: Pre-training of deep bidirectional transformers for language understanding. *arXiv preprint arXiv:1810.04805*, 2018.

[6] Aymeric Dieuleveut and Kumar Kshitij Patel. Communication trade-offs for local-sgd with large step size. *Advances in Neural Information Processing Systems*, 32:13601–13612, 2019.

[7] Yuri Ermoliev. Stochastic quasigradient methods. numerical techniques for stochastic optimization. *Springer Series in Computational Mathematics*, (10):141–185, 1988.

[8] Jonas Gehring, Michael Auli, David Grangier, Denis Yarats, and Yann N Dauphin. Convolutional sequence to sequence learning. In *International Conference on Machine Learning*, pages 1243–1252. PMLR, 2017.

[9] Saeed Ghadimi and Guanghui Lan. Stochastic first-and zeroth-order methods for nonconvex stochastic programming. *SIAM Journal on Optimization*, 23(4):2341–2368, 2013.

[10] Eduard Gorbunov, Marina Danilova, and Alexander Gasnikov. Stochastic optimization with heavy-tailed noise via accelerated gradient clipping. *arXiv preprint arXiv:2005.10785*, 2020.

[11] Eduard Gorbunov, Filip Hanzely, and Peter Richtárik. Local sgd: Unified theory and new efficient methods. In *International Conference on Artificial Intelligence and Statistics*, pages 3556–3564. PMLR, 2021.

[12] Priya Goyal, Piotr Dollár, Ross Girshick, Pieter Noordhuis, Lukasz Wesolowski, Aapo Kyrola, Andrew Tulloch, Yangqing Jia, and Kaiming He. Accurate, large minibatch sgd: Training imagenet in 1 hour. *arXiv preprint arXiv:1706.02677*, 2017.

[13] Farzin Haddadpour, Mohammad Mahdi Kamani, Mehrdad Mahdavi, and Viveck Cadambe. Local sgd with periodic averaging: Tighter analysis and adaptive synchronization. In *Advances in Neural Information Processing Systems*, pages 11080–11092, 2019.

[14] Elad Hazan, Kfir Y Levy, and Shai Shalev-Shwartz. Beyond convexity: Stochastic quasi-convex optimization. *arXiv preprint arXiv:1507.02030*, 2015.

[15] Kaiming He, Xiangyu Zhang, Shaoqing Ren, and Jian Sun. Deep residual learning for image recognition. In *Proceedings of the IEEE conference on computer vision and pattern recognition*, pages 770–778, 2016.

[16] Prateek Jain, Sham M Kakade, Rahul Kidambi, Praneeth Netrapalli, and Aaron Sidford. Parallelizing stochastic gradient descent for least squares regression: Mini-batching, averaging, and model misspecification. *Journal of Machine Learning Research*, 18:223–1, 2017.

[17] Peng Jiang and Gagan Agrawal. A linear speedup analysis of distributed deep learning with sparse and quantized communication. In *Advances in Neural Information Processing Systems*, pages 2525–2536, 2018.

[18] Peter Kairouz, H Brendan McMahan, Brendan Avent, Aurélien Bellet, Mehdi Bennis, Arjun Nitin Bhagoji, Kallista Bonawitz, Zachary Charles, Graham Cormode, Rachel Cummings, et al. Advances and open problems in federated learning. *arXiv preprint arXiv:1912.04977*, 2019.

[19] Sai Praneeth Karimireddy, Satyen Kale, Mehryar Mohri, Sashank Reddi, Sebastian Stich, and Ananda Theertha Suresh. Scaffold: Stochastic controlled averaging for federated learning. In *International Conference on Machine Learning*, pages 5132–5143. PMLR, 2020.

[20] Ahmed Khaled, Konstantin Mishchenko, and Peter Richtárik. Tighter theory for local sgd on identical and heterogeneous data. In *International Conference on Artificial Intelligence and Statistics*, pages 4519–4529. PMLR, 2020.

[21] Anastasia Koloskova, Nicolas Loizou, Sadra Boreiri, Martin Jaggi, and Sebastian Stich. A unified theory of decentralized sgd with changing topology and local updates. In *International Conference on Machine Learning*, pages 5381–5393. PMLR, 2020.

[22] Anastasia Koloskova, Sebastian U. Stich, and Martin Jaggi. Decentralized stochastic optimization and gossip algorithms with compressed communication. In *Proceedings of the 36th International Conference on Machine Learning, ICML 2019, 9-15 June 2019, Long Beach, California, USA*, pages 3478–3487, 2019.

[23] Alex Krizhevsky, Ilya Sutskever, and Geoffrey E Hinton. Imagenet classification with deep convolutional neural networks. In *Advances in neural information processing systems*, pages 1097–1105, 2012.

[24] Kfir Y Levy. The power of normalization: Faster evasion of saddle points. *arXiv preprint arXiv:1611.04831*, 2016.

[25] Tao Lin, Sebastian U Stich, Kumar Kshitij Patel, and Martin Jaggi. Don't use large mini-batches, use local sgd. *arXiv preprint arXiv:1808.07217*, 2018.

[26] Vien V Mai and Mikael Johansson. Stability and convergence of stochastic gradient clipping: Beyond lipschitz continuity and smoothness. *arXiv preprint arXiv:2102.06489*, 2021.

[27] Mitchell P. Marcus, Mary Ann Marcinkiewicz, and Beatrice Santorini. Building a large annotated corpus of english: The penn treebank. *Comput. Linguist.*, 19(2):313–330, June 1993.

[28] Ryan McDonald, Keith Hall, and Gideon Mann. Distributed training strategies for the structured perceptron. In *Human Language Technologies: The 2010 Annual Conference of the North American Chapter of the Association for Computational Linguistics*, pages 456–464. Association for Computational Linguistics, 2010.

[29] H Brendan McMahan, Eider Moore, Daniel Ramage, Seth Hampson, et al. Communication-efficient learning of deep networks from decentralized data. *AISTATS*, 2017.

[30] Aditya Krishna Menon, Ankit Singh Rawat, Sashank J Reddi, and Sanjiv Kumar. Can gradient clipping mitigate label noise? In *International Conference on Learning Representations*, 2019.

[31] Stephen Merity, Nitish Shirish Keskar, and Richard Socher. Regularizing and optimizing LSTM language models. In *International Conference on Learning Representations*, 2018.

[32] Yurii E Nesterov. Minimization methods for nonsmooth convex and quasiconvex functions. *Matekon*, 29:519–531, 1984.

[33] Razvan Pascanu, Tomas Mikolov, and Yoshua Bengio. Understanding the exploding gradient problem. corr abs/1211.5063 (2012). *arXiv preprint arXiv:1211.5063*, 2012.

[34] Razvan Pascanu, Tomas Mikolov, and Yoshua Bengio. On the difficulty of training recurrent neural networks. In *International conference on machine learning*, pages 1310–1318. PMLR, 2013.

[35] Matthew E Peters, Mark Neumann, Mohit Iyyer, Matt Gardner, Christopher Clark, Kenton Lee, and Luke Zettlemoyer. Deep contextualized word representations. *arXiv preprint arXiv:1802.05365*, 2018.

[36] Sashank Reddi, Zachary Charles, Manzil Zaheer, Zachary Garrett, Keith Rush, Jakub Konecny, Sanjiv Kumar, and H Brendan McMahan. Adaptive federated optimization. *ICLR*, 2021.

[37] Ohad Shamir and Nathan Srebro. Distributed stochastic optimization and learning. In *2014 52nd Annual Allerton Conference on Communication, Control, and Computing (Allerton)*, pages 850–857. IEEE, 2014.

[38] Naum Zuselevich Shor. *Minimization methods for non-differentiable functions*, volume 3. Springer Science & Business Media, 2012.

[39] David Silver, Aja Huang, Chris J Maddison, Arthur Guez, Laurent Sifre, George Van Den Driessche, Julian Schrittwieser, Ioannis Antonoglou, Veda Panneershelvam, Marc Lanctot, et al. Mastering the game of go with deep neural networks and tree search. *nature*, 529(7587):484, 2016.

[40] Sebastian U Stich. Local sgd converges fast and communicates little. *arXiv preprint arXiv:1805.09767*, 2018.

[41] Jianyu Wang and Gauri Joshi. Cooperative sgd: A unified framework for the design and analysis of communication-efficient sgd algorithms. *arXiv preprint arXiv:1808.07576*, 2018.

[42] Blake Woodworth, Brian Bullins, Ohad Shamir, and Nathan Srebro. The min-max complexity of distributed stochastic convex optimization with intermittent communication. *arXiv preprint arXiv:2102.01583*, 2021.

[43] Blake Woodworth, Kumar Kshitij Patel, and Nathan Srebro. Minibatch vs local sgd for heterogeneous distributed learning. *arXiv preprint arXiv:2006.04735*, 2020.

[44] Blake Woodworth, Kumar Kshitij Patel, Sebastian Stich, Zhen Dai, Brian Bullins, Brendan Mcmahan, Ohad Shamir, and Nathan Srebro. Is local sgd better than minibatch sgd? In *International Conference on Machine Learning*, pages 10334–10343. PMLR, 2020.

[45] Yang You, Igor Gitman, and Boris Ginsburg. Scaling sgd batch size to 32k for imagenet training. *arXiv preprint arXiv:1708.03888*, 6:12, 2017.

[46] Yang You, Jing Li, Sashank Reddi, Jonathan Hseu, Sanjiv Kumar, Srinadh Bhojanapalli, Xiaodan Song, James Demmel, Kurt Keutzer, and Cho-Jui Hsieh. Large batch optimization for deep learning: Training bert in 76 minutes. *arXiv preprint arXiv:1904.00962*, 2019.

[47] Hao Yu, Rong Jin, and Sen Yang. On the linear speedup analysis of communication efficient momentum SGD for distributed non-convex optimization. In *Proceedings of the 36th International Conference on Machine Learning, ICML 2019, 9-15 June 2019, Long Beach, California, USA*, pages 7184–7193, 2019.

[48] Hao Yu, Sen Yang, and Shenghuo Zhu. Parallel restarted sgd with faster convergence and less communication: Demystifying why model averaging works for deep learning. In *Proceedings of the AAAI Conference on Artificial Intelligence*, volume 33, pages 5693–5700, 2019.

[49] Honglin Yuan, Manzil Zaheer, and Sashank Reddi. Federated composite optimization. In *International Conference on Machine Learning*, pages 12253–12266. PMLR, 2021.

[50] Bohang Zhang, Jikai Jin, Cong Fang, and Liwei Wang. Improved analysis of clipping algorithms for non-convex optimization. *arXiv preprint arXiv:2010.02519*, 2020.

[51] Jingzhao Zhang, Tianxing He, Suvrit Sra, and Ali Jadbabaie. Why gradient clipping accelerates training: A theoretical justification for adaptivity. *arXiv preprint arXiv:1905.11881*, 2019.

[52] Xinwei Zhang, Xiangyi Chen, Mingyi Hong, Zhiwei Steven Wu, and Jinfeng Yi. Understanding clipping for federated learning: Convergence and client-level differential privacy. *arXiv preprint arXiv:2106.13673*, 2021.

[53] Xinwei Zhang, Mingyi Hong, Sairaj Dhople, Wotao Yin, and Yang Liu. Fedpd: A federated learning framework with optimal rates and adaptivity to non-iid data. *arXiv preprint arXiv:2005.11418*, 2020.

[54] Yuchen Zhang, John C Duchi, and Martin J Wainwright. Communication-efficient algorithms for statistical optimization. *The Journal of Machine Learning Research*, 14(1):3321–3363, 2013.

[55] Fan Zhou and Guojing Cong. On the convergence properties of a k-step averaging stochastic gradient descent algorithm for nonconvex optimization. *arXiv preprint arXiv:1708.01012*, 2017.

[56] Martin Zinkevich, Markus Weimer, Lihong Li, and Alex J Smola. Parallelized stochastic gradient descent. In *Advances in neural information processing systems*, pages 2595–2603, 2010.

Checklist

1. For all authors...
   (a) Do the main claims made in the abstract and introduction accurately reflect the paper's contributions and scope? [Yes]
   (b) Did you describe the limitations of your work? [Yes] See the Section 6
   (c) Did you discuss any potential negative societal impacts of your work? [N/A]
   (d) Have you read the ethics review guidelines and ensured that your paper conforms to them? [Yes]
2. If you are including theoretical results...
   (a) Did you state the full set of assumptions of all theoretical results? [Yes] See Section 3
   (b) Did you include complete proofs of all theoretical results? [Yes] See the Appendix
3. If you ran experiments...
   (a) Did you include the code, data, and instructions needed to reproduce the main experimental results (either in the supplemental material or as a URL)? [Yes] in the supplemental material
   (b) Did you specify all the training details (e.g., data splits, hyperparameters, how they were chosen)? [Yes] See the Section 5
   (c) Did you report error bars (e.g., with respect to the random seed after running experiments multiple times)? [No]
   (d) Did you include the total amount of compute and the type of resources used (e.g., type of GPUs, internal cluster, or cloud provider)? [Yes] See the Section 5
4. If you are using existing assets (e.g., code, data, models) or curating/releasing new assets...
   (a) If your work uses existing assets, did you cite the creators? [Yes]
   (b) Did you mention the license of the assets? [N/A]
   (c) Did you include any new assets either in the supplemental material or as a URL? [No]
   (d) Did you discuss whether and how consent was obtained from people whose data you're using/curating? [N/A]
   (e) Did you discuss whether the data you are using/curating contains personally identifiable information or offensive content? [N/A]
5. If you used crowdsourcing or conducted research with human subjects...
   (a) Did you include the full text of instructions given to participants and screenshots, if applicable? [N/A]
   (b) Did you describe any potential participant risks, with links to Institutional Review Board (IRB) approvals, if applicable? [N/A]
   (c) Did you include the estimated hourly wage paid to participants and the total amount spent on participant compensation? [N/A]

Appendix

A Properties of (L_0, L_1) functions and Useful Lemmas

Lemma 5 (Descent inequality in [50]). *Let f be (L_0, L_1)-smooth, and $c > 0$ be a constant. For any $\mathbf{x}_k$ and $\mathbf{x}_{k+1}$, as long as $\|\mathbf{x}_k - \mathbf{x}_{k+1}\| \leq c/L_1$, we have*

$$f(\mathbf{x}_{k+1}) \leq f(\mathbf{x}_k) + \langle \nabla f(\mathbf{x}_k), \mathbf{x}_{k+1} - \mathbf{x}_k \rangle + \frac{AL_0 + BL_1\|\nabla f(\mathbf{x}_k)\|}{2}\|\mathbf{x}_{k+1} - \mathbf{x}_k\|^2, \tag{5}$$

where $A = 1 + e^c - \frac{e^c - 1}{c}$ and $B = \frac{e^c - 1}{c}$.

Lemma 6 ([50]). *Let f be (L_0, L_1)-smooth, and $c > 0$ be a constant. For any $\mathbf{x}_k$ and $\mathbf{x}_{k+1}$, as long as $\|\mathbf{x}_k - \mathbf{x}_{k+1}\| \leq c/L_1$, we have*

$$\|\nabla f(\mathbf{x}_{k+1}) - \nabla f(\mathbf{x}_k)\| \leq (AL_0 + BL_1\|\nabla f(\mathbf{x}_k)\|)\,\|\mathbf{x}_{k+1} - \mathbf{x}_k\|, \tag{6}$$

where $A = 1 + e^c - \frac{e^c - 1}{c}$ and $B = \frac{e^c - 1}{c}$.

Lemma 7 ([50]). *Let $\mu \geq 0$ be a real constant. For any vectors $\mathbf{u}$ and $\mathbf{v}$,*

$$-\frac{\langle \mathbf{u}, \mathbf{v} \rangle}{\|\mathbf{v}\|} \leq -\mu\|\mathbf{u}\| - (1 - \mu)\|\mathbf{v}\| + (1 + \mu)\|\mathbf{v} - \mathbf{u}\|. \tag{7}$$

Lemma 8. *Suppose $\Lambda = diag(c_1, c_2, \ldots, c_d) \in \mathbb{R}^{d \times d}$ with $0 < c_i \leq 1$, $i = 1, \ldots, d$. Define $c_{\max} = \max(c_1, c_2, \ldots, c_d)$, $c_{\min} = \min(c_1, c_2, \ldots, c_d)$. Then we have*

$$\sqrt{c_{\min}}\|\mathbf{x}\|_2 \leq \|\mathbf{x}\|_\Lambda \leq \sqrt{c_{\max}}\|\mathbf{x}\|_2. \tag{8}$$

Proof. By definition, we have $\|\mathbf{x}\|_\Lambda = \sqrt{\mathbf{x}^\top \Lambda \mathbf{x}}$. Suppose $\mathbf{x} = (x_1, \ldots, x_d)$, then we have

$$\|\mathbf{x}\|_\Lambda^2 = c_1 x_1^2 + c_2 x_2^2 + \ldots + c_d x_d^2 \leq c_{\max}(x_1^2 + \ldots + x_d^2) = c_{\max}\|\mathbf{x}\|_2^2,$$
$$\|\mathbf{x}\|_\Lambda^2 = c_1 x_1^2 + c_2 x_2^2 + \ldots + c_d x_d^2 \geq c_{\min}(x_1^2 + \ldots + x_d^2) = c_{\min}\|\mathbf{x}\|_2^2.$$

Combining these inequalities and taking square root on both sides, the Lemma is proved. □

B Proof of Lemma 1

Proof. We first prove the 1-dimensional case. Let $g \in \mathbb{R}$ be a 1-dimensional random variable. Denote $\mu = \mathbb{E}[g]$ and $h(g)$ by the density of g over $\mathbb{R}$. Then by the assumption, we know that $h(\mu) \geq h(g)$ for any $g \in \mathbb{R}$, $h(\mu + x) = h(\mu - x)$ for any $x \in \mathbb{R}$ and $h(x) < h(y)$ if $|x - \mu| > |y - \mu|$ for $x, y \in \mathbb{R}$. We aim to prove that there exists $0 < c \leq 1$ such that $\mathbb{E}\left[g\mathbb{I}(|g| \leq \alpha)\right] = c \cdot \Pr(|g| \leq \alpha) \cdot \mu$. We consider the following three cases:

- $\mu = 0$. In this case, by the symmetry of probability density around its mean, we know that LHS $= \mathbb{E}\left[g\mathbb{I}(|g| \leq \alpha)\right] = 0 = c \cdot \Pr(|g| \leq \alpha) \cdot \mu =$ RHS, where $c = 1$.
- $\mu > 0$. We first prove that $\mathbb{E}\left[g\mathbb{I}(|g| \leq \alpha)\right]$ is positive. By definition, we have $\mathbb{E}\left[g\mathbb{I}(|g| \leq \alpha)\right] = \int_{-\alpha}^{0} gh(g)dg + \int_0^\alpha gh(g)dg := A_1 + A_2$. Note that $A_1 = \int_0^\alpha -gh(-g)dg$ and $h(g) > h(-g)$ for $g > 0$ (due to $\mu > 0$ and the monotonic decreasing property of the probability density), and then we have $A_1 + A_2 = \int_0^\alpha g(h(g) - h(-g))dg > 0$. Next, we show that there exists some $0 < c \leq 1$, such that $\mathbb{E}\left[g\mathbb{I}(|g| \leq \alpha)\right] = c \cdot \Pr(|g| \leq \alpha) \cdot \mu$. To show this we further consider two cases:
  - (i) $\alpha \leq \mu$. In this case, we have $\mathbb{E}\left[g\mathbb{I}(|g| \leq \alpha)\right] \leq \mu\mathbb{E}\left[\mathbb{I}(|g| \leq \alpha)\right] = \mu \cdot \Pr(|g| \leq \alpha)$. This fact together with $\mathbb{E}\left[g\mathbb{I}(|g| \leq \alpha)\right] > 0$ imply that there exists $0 < c \leq 1$ such that $\mathbb{E}\left[g\mathbb{I}(|g| \leq \alpha)\right] = c \cdot \Pr(|g| \leq \alpha) \cdot \mu$.
  - (ii) $\alpha > \mu$. In this case, we have

$$\mathbb{E}\left[g\mathbb{I}(|g| \leq \alpha)\right] = \int_{-\alpha}^{2\mu-\alpha} gh(g)dg + \int_{2\mu-\alpha}^{\mu} gh(g)dg + \int_{\mu}^{\alpha} gh(g)dg := A_1 + A_2 + A_3.$$

Define $\hat{g} = 2\mu - g$, then we have $A_2 = \int_\mu^\alpha (2\mu - \hat{g})h(2\mu - \hat{g})d\hat{g} = \int_\mu^\alpha (2\mu - \hat{g})h(\hat{g})d\hat{g}$ due to the symmetry around μ of the probability density. Hence we have $A_2 + A_3 = 2\mu \int_\mu^\alpha h(g)dg = \mu(\int_{2\mu-\alpha}^\mu h(g)dg + \int_\mu^\alpha h(g)dg)$ again due to the symmetry around μ of the probability density. As a result, we have

$$\mathbb{E}\left[g\mathbb{I}(|g| \le \alpha)\right] = \int_{-\alpha}^{2\mu-\alpha} gh(g)dg + \mu\left(\int_{2\mu-\alpha}^{\mu} h(g)dg + \int_{\mu}^{\alpha} h(g)dg\right) \le \mu \int_{-\alpha}^{\alpha} h(g)dg = \mu \cdot \Pr(|g| \le \alpha).$$

This fact together with $\mathbb{E}\left[g\mathbb{I}(|g| \le \alpha)\right] > 0$ imply that there exists $0 < c \le 1$ such that $\mathbb{E}\left[g\mathbb{I}(|g| \le \alpha)\right] = c \cdot \Pr(|g| \le \alpha) \cdot \mu$.

- $\mu < 0$. In this case we can use parallel argument as in the case of $\mu > 0$ to prove the same result.

Now we extend the proof from 1-dimensional to d-dimensional setting. Denote $\mathbf{g}_{[i]}$ by the i-th coordinate of $\mathbf{g}$, $\mu_i = \mathbb{E}\left[\mathbf{g}_{[i]}\right]$, where $i = 1, \ldots, d$, define $h(\mathbf{g})$ by the density of $\mathbf{g}$, and $\boldsymbol{\mu} = (\mu_1, \ldots, \mu_d)$. Then we have $h(\boldsymbol{\mu}) \ge h(\mathbf{g})$ for any $\mathbf{g} \in \mathbb{R}^d$, $h(\boldsymbol{\mu} + \mathbf{x}) = h(\boldsymbol{\mu} - \mathbf{x})$ for any $\mathbf{x} \in \mathbb{R}^d$ and $h(\mathbf{x}) < h(\mathbf{y})$ if $\|\mathbf{x} - \boldsymbol{\mu}\| > \|\mathbf{y} - \boldsymbol{\mu}\|$ with $\mathbf{x}, \mathbf{y} \in \mathbb{R}^d$. Without loss of generality, it suffices to show that there exists a constant $0 < c_1 \le 1$ such that $\mathbb{E}\left[\mathbf{g}_{[1]}\mathbb{I}(\|\mathbf{g}\| \le \alpha)\right] = c_1 \cdot \Pr(\|\mathbf{g}\| \le \alpha)\mathbb{E}\left[\mathbf{g}_{[1]}\right]$. Note that

$$\begin{aligned}
&\mathbb{E}\left[\mathbf{g}_{[1]}\mathbb{I}(\|\mathbf{g}\| \le \alpha)\right] = \int_{\|\mathbf{g}\| \le \alpha} \mathbf{g}_{[1]} h(\mathbf{g}) d\mathbf{g} \\
&= \int_{-\alpha}^{\alpha} \mathbf{g}_{[1]} \int_{\sum_{i=2}^d \mathbf{g}_{[i]}^2 \le \alpha^2 - \mathbf{g}_{[1]}^2} h(\mathbf{g}_{[1]}|\mathbf{g}_{[2]}, \ldots, \mathbf{g}_{[d]}) h(\mathbf{g}_{[2]}, \ldots, \mathbf{g}_{[d]}) d\mathbf{g}_{[1]}\mathbf{g}_{[2]} \cdots \mathbf{g}_{[d]} \\
&= \int_{-\alpha}^{0} \mathbf{g}_{[1]} \int_{\sum_{i=2}^d \mathbf{g}_{[i]}^2 \le \alpha^2 - \mathbf{g}_{[1]}^2} h(\mathbf{g}_{[1]}|\mathbf{g}_{[2]}, \ldots, \mathbf{g}_{[d]}) h(\mathbf{g}_{[2]}, \ldots, \mathbf{g}_{[d]}) d\mathbf{g}_{[1]}\mathbf{g}_{[2]} \cdots \mathbf{g}_{[d]} \\
&\quad + \int_{0}^{\alpha} \mathbf{g}_{[1]} \int_{\sum_{i=2}^d \mathbf{g}_{[i]}^2 \le \alpha^2 - \mathbf{g}_{[1]}^2} h(\mathbf{g}_{[1]}|\mathbf{g}_{[2]}, \ldots, \mathbf{g}_{[d]}) h(\mathbf{g}_{[2]}, \ldots, \mathbf{g}_{[d]}) d\mathbf{g}_{[1]}\mathbf{g}_{[2]} \cdots \mathbf{g}_{[d]} \\
&:= B_1 + B_2.
\end{aligned}$$

By change of variable (e.g., changing $\mathbf{g}_{[1]}$ by $-\mathbf{g}_{[1]}$), we know that

$$B_1 = \int_0^\alpha -\mathbf{g}_{[1]} \int_{\sum_{i=2}^d \mathbf{g}_{[i]}^2 \le \alpha^2 - \mathbf{g}_{[1]}^2} h(-\mathbf{g}_{[1]}|\mathbf{g}_{[2]}, \ldots, \mathbf{g}_{[d]}) h(\mathbf{g}_{[2]}, \ldots, \mathbf{g}_{[d]}) d\mathbf{g}_{[1]}\mathbf{g}_{[2]} \cdots \mathbf{g}_{[d]}.$$

As a result, we have

$$\begin{aligned}
&\mathbb{E}\left[\mathbf{g}_{[1]}\mathbb{I}(\|\mathbf{g}\| \le \alpha)\right] \\
&= \int_0^\alpha \mathbf{g}_{[1]} \int_{\sum_{i=2}^d \mathbf{g}_{[i]}^2 \le \alpha^2 - \mathbf{g}_{[1]}^2} (h(\mathbf{g}_{[1]}|\mathbf{g}_{[2]}, \ldots, \mathbf{g}_{[d]}) - h(-\mathbf{g}_{[1]}|\mathbf{g}_{[2]}, \ldots, \mathbf{g}_{[d]})) h(\mathbf{g}_{[2]}, \ldots, \mathbf{g}_{[d]}) d\mathbf{g}_{[1]}\mathbf{g}_{[2]} \cdots \mathbf{g}_{[d]} \\
&= \int_0^\alpha \mathbf{g}_{[1]} \int_{\sum_{i=2}^d \mathbf{g}_{[i]}^2 \le \alpha^2 - \mathbf{g}_{[1]}^2} (h(\mathbf{g}_{[1]}, \mathbf{g}_{[2]}, \ldots, \mathbf{g}_{[d]}) - h(-\mathbf{g}_{[1]}, \mathbf{g}_{[2]}, \ldots, \mathbf{g}_{[d]})) d\mathbf{g}_{[1]}\mathbf{g}_{[2]} \cdots \mathbf{g}_{[d]}.
\end{aligned}$$

Similar to the 1-dimensional analysis, we consider the following three cases:

- $\mu_1 = 0$. By the symmetry of the probability density around its mean, we know that $h(x_1, x_2, \ldots, x_d) = h(-x_1, x_2, \ldots, x_d)$, since $\mu_1 = 0$ and $\|(x_1, x_2, \ldots, x_d) - (\mu_1, \mu_2, \ldots, \mu_d)\| = \|(-x_1, x_2, \ldots, x_d) - (\mu_1, \mu_2, \ldots, \mu_d)\|$. Hence we know that LHS $= \mathbb{E}\left[\mathbf{g}_{[1]}\mathbb{I}(\|\mathbf{g}\| \le \alpha)\right] = 0 = c_1 \cdot \Pr(|\mathbf{g}| \le \alpha) \cdot \mathbb{E}\left[\mathbf{g}_{[1]}\right]$ for $c_1 = 1$.

- $\mu_1 > 0$. We first prove that $\mathbb{E}\left[\mathbf{g}_{[1]}\mathbb{I}(\|\mathbf{g}\| \le \alpha)\right]$ is also positive. In this case, by the symmetry of the probability density around its mean and the monotonically decreasing property of the density over the ℓ_2 distance between the mean and the random variable, we know that $h(x_1, x_2, \ldots, x_d) > h(-x_1, x_2, \ldots, x_d)$, since $\mu_1 > 0$ and $\|(x_1, x_2, \ldots, x_d) - (\mu_1, \mu_2, \ldots, \mu_d)\| < \|(-x_1, x_2, \ldots, x_d) - (\mu_1, \mu_2, \ldots, \mu_d)\|$ for any $0 \le x_1 \le \alpha$. Then we show that there exists some $0 < c_1 \le 1$ such that $\mathbb{E}\left[\mathbf{g}_{[1]}\mathbb{I}(\|\mathbf{g}\| \le \alpha)\right] = c_1 \cdot \Pr(\|g\| \le \alpha) \cdot \mathbb{E}\left[\mathbf{g}_{[1]}\right]$. We further consider two cases.

(i) $\alpha \leq \mu_1$. In this case, we have $\mathbb{E}\left[\mathbf{g}_{[1]}\mathbb{I}(\|\mathbf{g}\| \leq \alpha)\right] \leq \mu_1 \mathbb{E}\left[\mathbb{I}(\|\mathbf{g}\| \leq \alpha)\right]$, since $\|\mathbf{g}\| \leq \alpha$ implies $\mathbf{g}_{[1]} \leq \alpha \leq \mu_1$. This fact together with $\mathbb{E}\left[\mathbf{g}_{[1]}\mathbb{I}(\|\mathbf{g}\| \leq \alpha)\right] > 0$ imply that there exists $0 < c_1 \leq 1$ such that $\mathbb{E}\left[\mathbf{g}_{[1]}\mathbb{I}(\|\mathbf{g}\| \leq \alpha)\right] = c_1 \cdot \Pr(\|\mathbf{g}\| \leq \alpha) \cdot \mu_1$.

(ii) $\alpha > \mu_1$. In this case, we have

$$\begin{aligned}
\mathbb{E}\left[\mathbf{g}_{[1]}\mathbb{I}(\|\mathbf{g}\| \leq \alpha)\right] &= \int_{-\alpha}^{2\mu_1-\alpha} \mathbf{g}_{[1]} \int_{\sum_{i=2}^d \mathbf{g}_{[i]}^2 \leq \alpha^2 - \mathbf{g}_{[1]}^2} h(\mathbf{g}_{[1]}, \ldots, \mathbf{g}_{[d]}) d\mathbf{g}_{[1]} \ldots d\mathbf{g}_{[d]} \\
&\quad + \int_{2\mu_1-\alpha}^{\mu_1} \mathbf{g}_{[1]} \int_{\sum_{i=2}^d \mathbf{g}_{[i]}^2 \leq \alpha^2 - \mathbf{g}_{[1]}^2} h(\mathbf{g}_{[1]}, \ldots, \mathbf{g}_{[d]}) d\mathbf{g}_{[1]} \ldots d\mathbf{g}_{[d]} \\
&+ \int_{\mu_1}^{\alpha} \mathbf{g}_{[1]} \int_{\sum_{i=2}^d \mathbf{g}_{[i]}^2 \leq \alpha^2 - \mathbf{g}_{[1]}^2} h(\mathbf{g}_{[1]}, \ldots, \mathbf{g}_{[d]}) d\mathbf{g}_{[1]} \ldots d\mathbf{g}_{[d]} \\
&:= D_1 + D_2 + D_3.
\end{aligned}$$

Define $\widehat{\mathbf{g}}_{[1]} = 2\mu_1 - \mathbf{g}_{[1]}$, then we have

$$\begin{aligned}
D_2 &= \int_{\mu_1}^{\alpha} (2\mu_1 - \widehat{\mathbf{g}}_{[1]}) \int_{\sum_{i=2}^d \mathbf{g}_{[i]}^2 \leq \alpha^2 - \mathbf{g}_{[1]}^2} h(2\mu_1 - \widehat{\mathbf{g}}_{[1]}, \mathbf{g}_{[2]}, \ldots, \mathbf{g}_{[d]}) d\widehat{\mathbf{g}}_{[1]} \ldots \mathbf{g}_{[d]} \\
&= \int_{\mu_1}^{\alpha} (2\mu_1 - \widehat{\mathbf{g}}_{[1]}) \int_{\sum_{i=2}^d \mathbf{g}_{[i]}^2 \leq \alpha^2 - \mathbf{g}_{[1]}^2} h(\widehat{\mathbf{g}}_{[1]}, \mathbf{g}_{[2]}, \ldots, \mathbf{g}_{[d]}) d\widehat{\mathbf{g}}_{[1]} \ldots \mathbf{g}_{[d]},
\end{aligned}$$

where the second equality holds since the distribution is symmetric around $\boldsymbol{\mu}$ and $\|(2\mu_1 - x_1, x_2, \ldots, x_d) - (\mu_1, \mu_2, \ldots, \mu_d)\| = \|(x_1, x_2, \ldots, x_d) - (\mu_1, \mu_2, \ldots, \mu_d)\|$. As a result, we have

$$\begin{aligned}
D_2 + D_3 &= 2\mu_1 \int_{\mu_1}^{\alpha} \int_{\sum_{i=2}^d \mathbf{g}_{[i]}^2 \leq \alpha^2 - \mathbf{g}_{[1]}^2} h(\mathbf{g}_{[1]}, \mathbf{g}_{[2]}, \ldots, \mathbf{g}_{[d]}) d\mathbf{g}_{[1]} d\mathbf{g}_{[2]} \ldots d\mathbf{g}_{[d]} \\
&= \mu_1 \int_{2\mu_1-\alpha}^{\mu_1} \int_{\sum_{i=2}^d \mathbf{g}_{[i]}^2 \leq \alpha^2 - \mathbf{g}_{[1]}^2} h(\mathbf{g}_{[1]}, \mathbf{g}_{[2]}, \ldots, \mathbf{g}_{[d]}) d\mathbf{g}_{[1]} d\mathbf{g}_{[2]} \ldots d\mathbf{g}_{[d]} \\
&\quad + \mu_1 \int_{\mu_1}^{\alpha} \int_{\sum_{i=2}^d \mathbf{g}_{[i]}^2 \leq \alpha^2 - \mathbf{g}_{[1]}^2} h(\mathbf{g}_{[1]}, \mathbf{g}_{[2]}, \ldots, \mathbf{g}_{[d]}) d\mathbf{g}_{[1]} d\mathbf{g}_{[2]} \ldots d\mathbf{g}_{[d]},
\end{aligned}$$

where the second inequality holds again due to the symmetry of the probability density around $\boldsymbol{\mu}$. As a result we have

$$\begin{aligned}
\mathbb{E}\left[\mathbf{g}_{[1]}\mathbb{I}(\|\mathbf{g}\| \leq \alpha)\right] &= \int_{-\alpha}^{2\mu_1-\alpha} \mathbf{g}_{[1]} \int_{\sum_{i=2}^d \mathbf{g}_{[i]}^2 \leq \alpha^2 - \mathbf{g}_{[1]}^2} h(\mathbf{g}_{[1]}, \ldots, \mathbf{g}_{[d]}) d\mathbf{g}_{[1]} \ldots d\mathbf{g}_{[d]} \\
&+ \mu_1 \int_{2\mu_1-\alpha}^{\mu_1} \int_{\sum_{i=2}^d \mathbf{g}_{[i]}^2 \leq \alpha^2 - \mathbf{g}_{[1]}^2} h(\mathbf{g}_{[1]}, \ldots, \mathbf{g}_{[d]}) d\mathbf{g}_{[1]} \ldots d\mathbf{g}_{[d]} \\
&+ \mu_1 \int_{\mu_1}^{\alpha} \int_{\sum_{i=2}^d \mathbf{g}_{[i]}^2 \leq \alpha^2 - \mathbf{g}_{[1]}^2} h(\mathbf{g}_{[1]}, \ldots, \mathbf{g}_{[d]}) d\mathbf{g}_{[1]} \ldots d\mathbf{g}_{[d]} \\
&\leq \mu_1 \int_{-\alpha}^{\alpha} \int_{\sum_{i=2}^d \mathbf{g}_{[i]}^2 \leq \alpha^2 - \mathbf{g}_{[1]}^2} h(\mathbf{g}_{[1]}, \ldots, \mathbf{g}_{[d]}) d\mathbf{g}_{[1]} \ldots d\mathbf{g}_{[d]} \\
&= \mu_1 \cdot \int_{\|\mathbf{g}\| \leq \alpha} h(\mathbf{g}) d\mathbf{g} = \mu_1 \cdot \Pr(\|\mathbf{g}\| \leq \alpha).
\end{aligned}$$

This fact together with $\mathbb{E}\left[\mathbf{g}_{[1]}\mathbb{I}(\|\mathbf{g}\| \leq \alpha)\right] > 0$ imply that there exists $0 < c_1 \leq 1$ such that $\mathbb{E}\left[\mathbf{g}_{[1]}\mathbb{I}(\|\mathbf{g}\| \leq \alpha)\right] = c_1 \cdot \Pr(\|\mathbf{g}\| \leq \alpha) \cdot \mu_1$.

- $\mu_1 < 0$. In this case we can use parallel argument as in the case of $\mu_1 > 0$ to prove the same result.

Now we have proved that there exists a constant $0 < c_1 \leq 1$ such that $\mathbb{E}\left[\mathbf{g}_{[1]}\mathbb{I}(\|\mathbf{g}\| \leq \alpha)\right] = c_1 \cdot \Pr(\|\mathbf{g}\| \leq \alpha)\mathbb{E}\left[\mathbf{g}_{[1]}\right]$. Using the same argument we can show that there exists $0 < c_i \leq 1$ with $i = 1, \ldots, d$ such that $\mathbb{E}\left[\mathbf{g}_{[i]}\mathbb{I}(\|\mathbf{g}\| \leq \alpha)\right] = c_i \cdot \Pr(\|\mathbf{g}\| \leq \alpha)\mathbb{E}\left[\mathbf{g}_{[i]}\right]$. Hence the Lemma is proved.

□

C Proof of Theorem 1

During the proof of Theorem 1, we need the following simple fact for our algorithm.

Fact Recall the definition of $\bar{\mathbf{x}}_t = \frac{1}{N}\sum_{i=1}^N \mathbf{x}_t^i$ for a fixed iteration t, Algorithm 1 immediately gives us $\bar{\mathbf{x}}_{t+1} - \bar{\mathbf{x}}_t = -\frac{1}{N}\sum_{i=1}^N \min\left(\eta, \frac{\gamma}{\|\nabla F(\mathbf{x}_t^i;\xi_t^i)\|}\right)\nabla F(\mathbf{x}_t^i;\xi_t^i)$, and hence $\|\bar{\mathbf{x}}_{t+1} - \bar{\mathbf{x}}_t\|^2 \le \gamma^2$ holds for any t.

C.1 Proof of Lemma 2

Lemma 2 restated Under Assumption 1, Algorithm 1 ensures the following inequality almost surely:

$$\|\bar{\mathbf{x}}_t - \mathbf{x}_t^i\| \le 2\gamma I, \forall i, \forall t \tag{9}$$

Proof. Fix $t \ge 1$ and i. Note that Algorithm 1 calculates the node average every I iterations. Let $t_0 \le t$ be the largest multiple of I. Then we know $\bar{\mathbf{x}}_{t_0} = \mathbf{x}_{t_0}^i$ for all i (Note that $t - t_0 \le I$). We further notice that

$$\mathbf{x}_t^i = \bar{\mathbf{x}}_{t_0} - \sum_{\tau=t_0}^{t-1} \min\left(\eta, \frac{\gamma}{\|\nabla F(\mathbf{x}_\tau^i;\xi_\tau^i)\|}\right)\nabla F(\mathbf{x}_\tau^i;\xi_\tau^i).$$

By the definition of $\bar{\mathbf{x}}_t$, we have

$$\bar{\mathbf{x}}_t = \bar{\mathbf{x}}_{t_0} - \sum_{\tau=t_0}^{t-1}\frac{1}{N}\sum_{j=1}^N \min\left(\eta, \frac{\gamma}{\|\nabla F(\mathbf{x}_\tau^j;\xi_\tau^j)\|}\right)\nabla F(\mathbf{x}_\tau^j;\xi_\tau^j).$$

Thus, we have

$$\begin{aligned}
\|\bar{\mathbf{x}}_t - \mathbf{x}_t^i\|^2 &= \left\|\sum_{\tau=t_0}^{t-1} \min\left(\eta, \frac{\gamma}{\|\nabla F(\mathbf{x}_\tau^i;\xi_\tau^i)\|}\right)\nabla F(\mathbf{x}_\tau^i,\xi_\tau^i) - \sum_{\tau=t_0}^{t-1}\frac{1}{N}\sum_{j=1}^N \min\left(\eta, \frac{\gamma}{\|\nabla F(\mathbf{x}_\tau^j,\xi_\tau^j)\|}\right)\nabla F(\mathbf{x}_\tau^j;\xi_\tau^j)\right\|^2 \\
&\le 2\left\|\sum_{\tau=t_0}^{t-1} \min\left(\eta, \frac{\gamma}{\|\nabla F(\mathbf{x}_\tau^i;\xi_\tau^i)\|}\right)\nabla F(\mathbf{x}_\tau^i;\xi_\tau^i)\right\|^2 + 2\left\|\sum_{\tau=t_0}^{t-1}\frac{1}{N}\sum_{j=1}^N \min\left(\eta, \frac{\gamma}{\|\nabla F(\mathbf{x}_\tau^j;\xi_\tau^j)\|}\right)\nabla F(\mathbf{x}_\tau^j;\xi_\tau^j)\right\|^2 \\
&\le 2(t-t_0)\sum_{\tau=t_0}^{t-1}\left\|\min\left(\eta, \frac{\gamma}{\|\nabla F(\mathbf{x}_\tau^i;\xi_\tau^i)\|}\right)\nabla F(\mathbf{x}_\tau^i;\xi_\tau^i)\right\|^2 + \frac{2(t-t_0)}{N^2}\sum_{\tau=t_0}^{t-1}\left\|\sum_{j=1}^N \min\left(\eta, \frac{\gamma}{\|\nabla F(\mathbf{x}_\tau^j;\xi_\tau^j)\|}\right)\nabla F(\mathbf{x}_\tau^j;\xi_\tau^j)\right\|^2 \\
&\le 2\gamma^2(t-t_0)\sum_{\tau=t_0}^{t-1}\left\|\frac{\nabla F(\mathbf{x}_\tau^i,\xi_\tau^i)}{\|\nabla F(\mathbf{x}_\tau^i;\xi_\tau^i)\|}\right\|^2 + \frac{2(t-t_0)}{N^2}N\sum_{\tau=t_0}^{t-1}\sum_{j=1}^N \gamma^2\left\|\frac{\nabla F(\mathbf{x}_\tau^j;\xi_\tau^j)}{\|\nabla F(\mathbf{x}_\tau^j,\xi_\tau^j)\|}\right\|^2 \\
&\le 2\gamma^2 I^2 + \frac{2(t-t_0)}{N}\sum_{\tau=t_0+1}^{t}\sum_{j=1}^N \gamma^2 \\
&\le 4\gamma^2 I^2.
\end{aligned} \tag{10}$$

where the first inequality holds since $\|\sum_{j=1}^K \mathbf{z}_j\|^2 \le K\sum_{j=1}^K \|\mathbf{z}_j\|^2$ for any K vectors $\mathbf{z}_1, \ldots, \mathbf{z}_K$. Taking the square root on both sides, we obtain the desired result. □

C.2 Proof of Lemma 3

Note that $J(t) = \{i \in [N] \mid \|\nabla F(\mathbf{x}_t^i, \xi_t^i)\| \ge \frac{\gamma}{\eta}\}$.

Lemma 3 restated If $AL_0\eta \le 1/2$ and $2\gamma I \le c/L_1$ for some $c > 0$, then we have

$$
\begin{aligned}
&\mathbb{E}\left[f(\bar{\mathbf{x}}_{t+1}) - f(\bar{\mathbf{x}}_t)\right] \\
\le &\frac{1}{N}\mathbb{E}\sum_{i\in J(t)}\left[-\frac{2\gamma}{5}\|\nabla f(\bar{\mathbf{x}}_t)\| - \frac{3\gamma^2}{5\eta} + \frac{7\gamma}{5}\|\nabla F(\mathbf{x}_t^i;\xi_t^i) - \nabla f(\bar{\mathbf{x}}_t)\| + AL_0\gamma^2 + \frac{BL_1\gamma^2\|\nabla f(\bar{\mathbf{x}}_t)\|}{2} + \frac{50AL_0\eta^2\sigma^2}{N}\right] \\
+ &\frac{1}{N}\mathbb{E}\sum_{i\in \bar{J}(t)}\left[-\frac{\eta c_{\min}}{2}\|\nabla f(\bar{\mathbf{x}}_t)\|^2 + 4\gamma^2 I^2 A^2 L_0^2\eta + 4\gamma^2 I^2 B^2 L_1^2\eta\|\nabla f(\bar{\mathbf{x}}_t)\|^2 + \frac{50AL_0\eta^2\sigma^2}{N} + \frac{BL_1\gamma^2\|\nabla f(\bar{\mathbf{x}}_t)\|}{2}\right],
\end{aligned}
$$

where $A = 1 + e^c - \frac{e^c-1}{c}$ and $B = \frac{e^c-1}{c}$.

Proof. By the (L_0, L_1)-smoothness and invoking Lemma 5 and noting that $\|\bar{\mathbf{x}}_{t+1} - \bar{\mathbf{x}}_t\| \le \gamma$ for any t, we have

$$
\begin{aligned}
&f(\bar{\mathbf{x}}_{t+1}) - f(\bar{\mathbf{x}}_t) \le \langle \nabla f(\bar{\mathbf{x}}_t), \bar{\mathbf{x}}_{t+1} - \bar{\mathbf{x}}_t\rangle + \frac{(AL_0 + BL_1\|\nabla f(\bar{\mathbf{x}}_t)\|)}{2}\|\bar{\mathbf{x}}_{t+1} - \bar{\mathbf{x}}_t\|^2 \\
\le &-\gamma\left\langle \frac{1}{N}\sum_{i\in J(t)}\frac{\nabla F(\mathbf{x}_t^i;\xi_t^i)}{\|\nabla F(\mathbf{x}_t^i;\xi_t^i)\|}, \nabla f(\bar{\mathbf{x}}_t)\right\rangle - \eta\left\langle \frac{1}{N}\sum_{i\in \bar{J}(t)}\nabla F(\mathbf{x}_t^i;\xi_t^i), \nabla f(\bar{\mathbf{x}}_t)\right\rangle \\
&+ \frac{AL_0}{2}\|\bar{\mathbf{x}}_{t+1} - \bar{\mathbf{x}}_t\|^2 + \frac{BL_1\|\nabla f(\bar{\mathbf{x}}_t)\|\gamma^2}{2}.
\end{aligned} \tag{11}
$$

For each iteration t, we first consider the case where $i \in J(t)$, i.e. $\|\nabla F(\mathbf{x}_t^i;\xi_t^i)\| \ge \frac{\gamma}{\eta}$. We use Lemma 7 with $\mu = \frac{2}{5}$ to obtain the following result

$$
-\gamma\frac{\langle \nabla F(\mathbf{x}_t^i;\xi_t^i), \nabla f(\bar{\mathbf{x}}_t)\rangle}{\|\nabla F(\mathbf{x}_t^i;\xi_t^i)\|} \le -\frac{2\gamma}{5}\|\nabla f(\bar{\mathbf{x}}_t)\| - \frac{3\gamma^2}{5\eta} + \frac{7\gamma}{5}\|\nabla F(\mathbf{x}_t^i;\xi_t^i) - \nabla f(\bar{\mathbf{x}}_t)\|. \tag{12}
$$

Taking the summation over $i \in J(t)$, we have

$$
-\gamma\left\langle \frac{1}{N}\sum_{i\in J(t)}\frac{\nabla F(\mathbf{x}_t^i;\xi_t^i)}{\|\nabla F(\mathbf{x}_t^i;\xi_t^i)\|}, \nabla f(\bar{\mathbf{x}}_t)\right\rangle \le \frac{1}{N}\sum_{i\in J(t)}\left[-\frac{2\gamma}{5}\|\nabla f(\bar{\mathbf{x}}_t)\| - \frac{3\gamma^2}{5\eta} + \frac{7\gamma}{5}\|\nabla F(\mathbf{x}_t^i;\xi_t^i) - \nabla f(\bar{\mathbf{x}}_t)\|\right]. \tag{13}
$$

Next, we consider the case in which $i \in \bar{J}(t)$, i.e., $\|\nabla F(\mathbf{x}_t^i,\xi_t^i)\| \le \frac{\gamma}{\eta}$ at fixed iteration t. Denote by $\xi^{[t-1]}$ the σ-algebra generated by all random variables until $(t-1)$-th iteration, i.e., $\xi^{[t-1]} = \sigma(\xi_0^1, \ldots, \xi_0^N, \xi_1^1, \ldots, \xi_1^N, \ldots, \xi_{t-1}^1, \ldots, \xi_{t-1}^N)$.

Define $p_t^i = \Pr(\|\nabla F(\mathbf{x}_t^i;\xi_t^i)\| \le \gamma/\eta \mid \xi^{[t-1]}) = \Pr(i \in \bar{J}(t) \mid \xi^{[t-1]})$, and denote $\mathbb{E}_t[\cdot] = \mathbb{E}[\cdot \mid \xi^{[t-1]}]$. We notice that

$$
\begin{aligned}
&-\eta\mathbb{E}_t\left\langle \frac{1}{N}\sum_{i\in \bar{J}(t)}\nabla F(\mathbf{x}_t^i;\xi_t^i), \frac{\mathbb{E}_t\left[|\bar{J}(t)|\right]}{N}\nabla f(\bar{\mathbf{x}}_t)\right\rangle \\
&= -\eta\left\langle \mathbb{E}_t\left[\frac{1}{N}\sum_{i\in \bar{J}(t)}\nabla F(\mathbf{x}_t^i;\xi_t^i)\right], \frac{\mathbb{E}_t\left[|\bar{J}(t)|\right]}{N}\nabla f(\bar{\mathbf{x}}_t)\right\rangle \\
&= -\eta\left\langle \mathbb{E}_t\left[\frac{1}{N}\sum_{i=1}^N\nabla F(\mathbf{x}_t^i;\xi_t^i)\mathbb{I}(i \in \bar{J}(t))\right], \frac{\mathbb{E}_t\left[|\bar{J}(t)|\right]}{N}\nabla f(\bar{\mathbf{x}}_t)\right\rangle \\
&\overset{(a)}{=} -\eta\left\langle \frac{1}{N}\sum_{i=1}^N p_t^i\Lambda\nabla f(\mathbf{x}_t^i), \frac{\mathbb{E}_t\left[|\bar{J}(t)|\right]}{N}\nabla f(\bar{\mathbf{x}}_t)\right\rangle = -\eta\left\langle \frac{1}{N}\sum_{i=1}^N p_t^i\nabla f(\mathbf{x}_t^i), \frac{\mathbb{E}_t\left[|\bar{J}(t)|\right]}{N}\nabla f(\bar{\mathbf{x}}_t)\right\rangle_\Lambda \\
&\overset{(b)}{=} -\frac{\eta}{2}\left[\left\|\frac{\mathbb{E}_t\left[|\bar{J}(t)|\right]}{N}\nabla f(\bar{\mathbf{x}}_t)\right\|_\Lambda^2 + \left\|\frac{1}{N}\sum_{i=1}^N p_t^i\nabla f(\mathbf{x}_t^i)\right\|_\Lambda^2 - \left\|\frac{1}{N}\sum_{i=1}^N p_t^i\nabla f(\mathbf{x}_t^i) - \frac{\mathbb{E}_t\left[|\bar{J}(t)|\right]}{N}\nabla f(\bar{\mathbf{x}}_t)\right\|_\Lambda^2\right],
\end{aligned} \tag{14}
$$

where (a) holds due to Lemma 1, $p_t^i = \Pr(\|\nabla F(\mathbf{x}_t^i;\xi_t^i)\| \le \gamma/\eta \mid \xi^{[t-1]})$, $\|\mathbf{x}\|_\Lambda = \|\Lambda^{1/2}\mathbf{x}\|_2$ and $\langle \mathbf{x},\mathbf{y}\rangle_\Lambda = \mathbf{x}^\top \Lambda \mathbf{y}$ for any $\mathbf{x},\mathbf{y}$; (b) holds since $\langle \mathbf{x}_1,\mathbf{x}_2\rangle_\Lambda = \frac{1}{2}\left(\|\mathbf{x}_1\|_\Lambda^2 + \|\mathbf{x}_2\|_\Lambda^2 - \|\mathbf{x}_1-\mathbf{x}_2\|_\Lambda^2\right)$ for any two vectors $\mathbf{x}_1,\mathbf{x}_2$. We further bound the RHS of (14) as the following:

$$
\begin{aligned}
\text{RHS of (14)} &= -\frac{\eta(\mathbb{E}_t|\bar{J}(t)|)^2}{2N^2}\|\nabla f(\bar{\mathbf{x}}_t)\|_\Lambda^2 - \frac{\eta}{2}\left\|\frac{1}{N}\sum_{i=1}^N p_t^i \nabla f(\mathbf{x}_t^i)\right\|_\Lambda^2 + \frac{\eta}{2}\left\|\frac{1}{N}\sum_{i=1}^N p_t^i(\nabla f(\bar{\mathbf{x}}_t) - \nabla f(\mathbf{x}_t^i))\right\|_\Lambda^2 \\
&\overset{(c)}{\le} -\frac{\eta(\mathbb{E}_t|\bar{J}(t)|)^2}{2N^2}\|\nabla f(\bar{\mathbf{x}}_t)\|_\Lambda^2 - \frac{\eta}{2}\left\|\frac{1}{N}\sum_{i=1}^N p_t^i \nabla f(\mathbf{x}_t^i)\right\|_\Lambda^2 + \frac{\eta}{2}\frac{(\mathbb{E}_t|\bar{J}(t)|)^2}{N^2}\cdot\max_i\left\|(\nabla f(\bar{\mathbf{x}}_t) - \nabla f(\mathbf{x}_t^i))\right\|_\Lambda^2 \\
&\overset{(d)}{\le} -\frac{\eta(\mathbb{E}_t|\bar{J}(t)|)^2}{2N^2}\|\nabla f(\bar{\mathbf{x}}_t)\|_\Lambda^2 - \frac{\eta}{2}\left\|\frac{1}{N}\sum_{i=1}^N p_t^i \nabla F(\mathbf{x}_t^i)\right\|_\Lambda^2 + \frac{\eta}{2}\frac{(\mathbb{E}_t|\bar{J}(t)|)^2}{N^2}\left[4\gamma^2 I^2 c_{\max}\left(AL_0 + BL_1\|\nabla f(\bar{\mathbf{x}}_t)\|\right)^2\right] \\
&\overset{(e)}{\le} -\frac{\eta c_{\min}(\mathbb{E}_t|\bar{J}(t)|)^2}{2N^2}\|\nabla f(\bar{\mathbf{x}}_t)\|^2 - \frac{\eta}{2}\left\|\frac{1}{N}\sum_{i=1}^N p_t^i \nabla f(\mathbf{x}_t^i)\right\|_\Lambda^2 \\
&\quad + \frac{(\mathbb{E}_t|\bar{J}(t)|)^2}{N^2}\left[4\gamma^2 I^2 A^2 c_{\max} L_0^2\eta + 4\gamma^2 I^2 B^2 c_{\max} L_1^2 \eta\|\nabla f(\bar{\mathbf{x}}_t)\|^2\right],
\end{aligned}
\tag{15}
$$

where (c) holds due to $\sum_{i=1}^N p_t^i = \mathbb{E}_t|\bar{J}(t)|$, and $\|\frac{1}{N}\sum_{i=1}^N p_t^i \mathbf{a}_t^i\|_\Lambda \le \frac{1}{N}\sum_{i=1}^N p_t^i\|\mathbf{a}_t^i\|_\Lambda \le \frac{1}{N}\sum_{i=1}^N p_t^i \cdot \max_i \|\mathbf{a}_t^i\|_\Lambda$ with $\mathbf{a}_t^i = \nabla f(\bar{\mathbf{x}}_t) - \nabla f(\mathbf{x}_t^i)$; (d) holds due to Lemma 2, Lemma 6, and Lemma 8, (e) holds since $(a+b)^2 \le 2a^2 + 2b^2$ and Lemma 8.

Divide both sides of (14) and (15) by $\frac{\mathbb{E}_t\left[|\bar{J}(t)|\right]}{N}$ we have:

$$
\begin{aligned}
&-\eta\mathbb{E}_t\left\langle \frac{1}{N}\sum_{i\in\bar{J}(t)}\nabla F(\mathbf{x}_t^i;\xi_t^i), \nabla f(\bar{\mathbf{x}}_t)\right\rangle \le -\frac{\eta c_{\min}\mathbb{E}_t\left[|\bar{J}(t)|\right]}{2N}\|\nabla f(\bar{\mathbf{x}}_t)\|^2 - \frac{\eta N}{2\mathbb{E}_t\left[|\bar{J}(t)|\right]}\left\|\frac{1}{N}\sum_{i=1}^N p_t^i\nabla f(\mathbf{x}_t^i)\right\|_\Lambda^2 \\
&+ \frac{\mathbb{E}_t\left[|\bar{J}(t)|\right]}{N}\left[4\gamma^2 I^2 A^2 c_{\max} L_0^2\eta + 4\gamma^2 I^2 B^2 c_{\max} L_1^2\eta\|\nabla f(\bar{\mathbf{x}}_t)\|^2\right].
\end{aligned}
\tag{16}
$$

Next, we compute $\mathbb{E}_t\|\bar{\mathbf{x}}_{t+1} - \bar{\mathbf{x}}_t\|^2$. By definition, we have

$$
\begin{aligned}
&\mathbb{E}_t\|\bar{\mathbf{x}}_{t+1} - \bar{\mathbf{x}}_t\|^2 = \mathbb{E}_t\left\|\frac{1}{N}\sum_{i=1}^N \min\left(\eta, \frac{\gamma}{\|\nabla F(\mathbf{x}_t^i;\xi_t^i)\|}\right)\nabla F(\mathbf{x}_t^i;\xi_t^i)\right\|^2 \\
&= \frac{1}{N^2}\mathbb{E}_t\left\|\sum_{i=1}^N \min\left(\eta, \frac{\gamma}{\|\nabla F(\mathbf{x}_t^i;\xi_t^i)\|}\right)\nabla F(\mathbf{x}_t^i,\xi_t^i)\right\|^2 = \frac{1}{N^2}\mathbb{E}_t\left\|\gamma\sum_{i\in J(t)}\frac{\nabla F(\mathbf{x}_t^i;\xi_t^i)}{\|\nabla F(\mathbf{x}_t^i;\xi_t^i)\|} + \eta\sum_{i\in\bar{J}(t)}\nabla F(\mathbf{x}_t^i;\xi_t^i)\right\|^2 \\
&\le 2\gamma^2\mathbb{E}_t\left\|\frac{1}{N}\sum_{i\in J(t)}\frac{\nabla F(\mathbf{x}_t^i;\xi_t^i)}{\|\nabla F(\mathbf{x}_t^i;\xi_t^i)\|}\right\|^2 + 2\eta^2\mathbb{E}_t\left\|\frac{1}{N}\sum_{i=1}^N\nabla F(\mathbf{x}_t^i;\xi_t^i)\mathbb{I}\left(i\in\bar{J}(t)\right)\right\|^2 \\
&\le \frac{2\gamma^2}{N^2}\mathbb{E}_t\left\|\sum_{i\in J(t)}\frac{\nabla F(\mathbf{x}_t^i;\xi_t^i)}{\|\nabla F(\mathbf{x}_t^i;\xi_t^i)\|}\right\|^2 + 2\eta^2\mathbb{E}_t\left\|\frac{1}{N}\sum_{i=1}^N\nabla F(\mathbf{x}_t^i;\xi_t^i)\mathbb{I}\left(i\in\bar{J}(t)\right) - \mathbb{E}_t\left[\frac{1}{N}\sum_{i=1}^N\nabla F(\mathbf{x}_t^i;\xi_t^i)\mathbb{I}\left(i\in\bar{J}(t)\right)\right]\right\|^2 \\
&\quad + 2\eta^2\left\|\mathbb{E}_t\left(\frac{1}{N}\sum_{i=1}^N\nabla F(\mathbf{x}_t^i;\xi_t^i)\mathbb{I}\left(i\in\bar{J}(t)\right)\right)\right\|^2 \\
&\overset{(a)}{\le} \frac{2\gamma^2\mathbb{E}_t\left[|J(t)|^2\right]}{N^2} + \frac{100\eta^2\sigma^2}{N} + 2\eta^2\left\|\mathbb{E}_t\left(\frac{1}{N}\sum_{i=1}^N\nabla F(\mathbf{x}_t^i;\xi_t^i)\mathbb{I}\left(i\in\bar{J}(t)\right)\right)\right\|^2 \\
&\overset{(b)}{=} \frac{2\gamma^2\mathbb{E}_t\left[|J(t)|^2\right]}{N^2} + \frac{100\eta^2\sigma^2}{N} + 2\eta^2\left\|\frac{1}{N}\sum_{i=1}^N p_t^i\Lambda\nabla f(\mathbf{x}_t^i)\right\|^2,
\end{aligned}
\tag{17}
$$

where (a) holds since we have $\mathbb{E}_t \left\|\nabla F(\mathbf{x}_t^i;\xi_t^i)\mathbb{I}(i\in\bar{J}(t)) - \mathbb{E}_t\left[\nabla F(\mathbf{x}_t^i;\xi_t^i)\mathbb{I}(i\in\bar{J}(t))\right]\right\|^2 \leq 100\sigma^2$, which is further due to $\|\nabla F(\mathbf{x}_t^i;\xi_t^i)\mathbb{I}(i\in\bar{J}(t))\| \leq \gamma/\eta = 5\sigma$ almost surely; (b) holds due to Lemma 1.

Substituting (13), (16), and (17) into (11) yields

$$
\begin{aligned}
&\mathbb{E}_t[f(\bar{\mathbf{x}}_{t+1}) - f(\bar{\mathbf{x}}_t)] \\
&\leq \frac{1}{N}\mathbb{E}_t \sum_{i\in J(t)} \left[-\frac{2\gamma}{5}\|\nabla f(\bar{\mathbf{x}}_t)\| - \frac{3\gamma^2}{5\eta} + \frac{7\gamma}{5}\left\|\nabla F(\mathbf{x}_t^i;\xi_t^i) - \nabla f(\bar{\mathbf{x}}_t)\right\|\right] - \frac{\eta c_{\min}\mathbb{E}_t|\bar{J}(t)|}{2N}\|\nabla f(\bar{\mathbf{x}}_t)\|^2 \\
&- \frac{\eta}{2}\frac{N}{\mathbb{E}_t|\bar{J}(t)|}\left\|\frac{1}{N}\sum_{i=1}^N p_t^i \nabla F(\mathbf{x}_t^i)\right\|_\Lambda^2 + \frac{\mathbb{E}_t|\bar{J}(t)|}{N}\left[4\gamma^2 I^2 A^2 c_{\max} L_0^2\eta + 4\gamma^2 I^2 B^2 c_{\max} L_1^2 \eta \|\nabla f(\bar{\mathbf{x}}_t)\|^2\right] \\
&+ \frac{AL_0\gamma^2\mathbb{E}_t\left[|J(t)|^2\right]}{N^2} + \frac{50AL_0\eta^2\sigma^2}{N} + AL_0\eta^2\left\|\frac{1}{N}\sum_{i=1}^N p_t^i \Lambda\nabla F(\mathbf{x}_t^i)\right\|^2 + \frac{BL_1\gamma^2\|\nabla f(\bar{\mathbf{x}}_t)\|}{2} \\
&\leq \frac{1}{N}\mathbb{E}_t \sum_{i\in J(t)}\left[-\frac{2\gamma}{5}\|\nabla f(\bar{\mathbf{x}}_t)\| - \frac{3\gamma^2}{5\eta} + \frac{7\gamma}{5}\|\nabla F(\mathbf{x}_t^i;\xi_t^i) - \nabla f(\bar{\mathbf{x}}_t)\| + AL_0\gamma^2 + \frac{BL_1\gamma^2\|\nabla f(\bar{\mathbf{x}}_t)\|}{2} + \frac{50AL_0\eta^2\sigma^2}{N}\right] \\
&+ \frac{1}{N}\mathbb{E}_t \sum_{i\in\bar{J}(t)}\left[-\frac{\eta c_{\min}}{2}\|\nabla f(\bar{\mathbf{x}}_t)\|^2 + 4\gamma^2 I^2 A^2 L_0^2\eta + 4\gamma^2 I^2 B^2 L_1^2\eta\|\nabla f(\bar{\mathbf{x}}_t)\|^2 + \frac{50AL_0\eta^2\sigma^2}{N} + \frac{BL_1\gamma^2\|\nabla f(\bar{\mathbf{x}}_t)\|}{2}\right],
\end{aligned}
\tag{18}
$$

where the last inequality holds since $AL_0\eta \leq \frac{1}{2}$, $|\bar{J}(t)| \leq N$ and $|J(t)| \leq N$ almost surely, $\mathbb{E}_t\left[|J(t)|^2\right] \leq N\mathbb{E}_t\left[|J(t)|\right]$, and all diagonal entries of Λ are positive and not greater than 1, and $0 < c_{\max} \leq 1$.

Take the total expectation over inequality (18) completes the proof. □

C.3 Proof of Lemma 4

Lemma 4 restated Suppose Assumption 1 holds. If $2\gamma I \leq c/L_1$ for some $c > 0$, then we obtain

$$\|\nabla F(\mathbf{x}_t^i;\xi_t^i) - \nabla f(\bar{\mathbf{x}}_t)\| \leq \sigma + 2\gamma I(AL_0 + BL_1\|\nabla f(\bar{\mathbf{x}}_t)\|) \quad \text{almost surely,}$$

where $A = 1 + e^c - \frac{e^c-1}{c}$ and $B = \frac{e^c-1}{c}$.

Proof. By using triangular inequality and Lemma 6, we obtain

$$
\begin{aligned}
&\|\nabla F(\mathbf{x}_t^i;\xi_t^i) - \nabla f(\bar{\mathbf{x}}_t)\| \leq \|\nabla F(\mathbf{x}_t^i;\xi_t^i) - \nabla f(\mathbf{x}_t^i)\| + \|\nabla f(\mathbf{x}_t^i) - \nabla f(\bar{\mathbf{x}}_t)\| \\
&\leq \sigma + 2\gamma I(AL_0 + BL_1\|\nabla f(\bar{\mathbf{x}}_t)\|).
\end{aligned}
$$

□

C.4 Main Proof of Theorem 1

Proof. We consider $0 < \epsilon \leq \min(\frac{AL_0}{BL_1}, 0.1)$ be a small enough constant and assume $\sigma \geq 1$. Choose $N \leq \min\{\frac{1}{\epsilon}, \frac{14AL_0}{5BL_1\epsilon}\}$, $\gamma \leq c_{\min}\frac{N\epsilon}{28\sigma}\min\{\frac{\epsilon}{AL_0}, \frac{1}{BL_1}\}$, ratio $\gamma/\eta = 5\sigma$ and $I \leq \sqrt{\frac{1}{c_{\min}}}\frac{\sigma}{N\epsilon}$, we first check several important conditions which were used in previous Lemmas and we will use in our later proof.

$$AL_0\eta \leq AL_0\frac{c_{\min}N\epsilon}{5\sigma\cdot 28\sigma}\frac{\epsilon}{AL_0} \overset{(a)}{\leq} \frac{c_{\min}\epsilon}{140\sigma^2} \overset{(b)}{\leq} \frac{\epsilon}{140} \leq \frac{1}{2},$$

where (a) holds because of $N\epsilon \leq 1$ and (b) is true due to $\sigma \geq 1$ and $c_{\min} \leq 1$. Note that $N\epsilon \leq 1$, $\sigma \geq 1$, $A \geq 1$, $B \geq 1$, and so we have

$$2\gamma I \leq 2c_{\min}\frac{N\epsilon}{28\sigma}\frac{1}{BL_1}\cdot\sqrt{\frac{1}{c_{\min}}}\frac{7\sigma}{N\epsilon} \leq \frac{1}{2L_1} = \frac{c}{L_1},$$

where $c = \frac{1}{2}$. Recall the descent inequality (Lemma 5), we can explicitly define

$$A = 1 + e^{1/2} - \frac{e^{1/2} - 1}{1/2},$$
$$B = \frac{e^{1/2} - 1}{1/2}.$$

We can show that our choice of ϵ guarantees that $\frac{\epsilon}{AL_0} \leq \frac{1}{BL_1}$. Then, the upper bound of the parameter γ becomes $\frac{c_{\min} N \epsilon^2}{28 A L_0 \sigma}$. Based on Lemma 3 and Lemma 4, we take summation over t and obtain

$$\begin{aligned}
&\mathbb{E}\left[\sum_{t=0}^{T-1} f(\bar{\mathbf{x}}_{t+1}) - f(\bar{\mathbf{x}}_t)\right] \\
&\overset{(a)}{\leq} \frac{1}{N}\sum_{t=0}^{T-1}\mathbb{E}\sum_{i\in J(t)}[P_1 + P_2\|\nabla f(\bar{\mathbf{x}}_t)\|] + \\
&\quad \frac{1}{N}\sum_{t=0}^{T-1}\mathbb{E}\sum_{i\in \bar{J}(t)}\left[-\frac{\eta c_{\min}}{2}\|\nabla f(\bar{\mathbf{x}}_t)\|^2 + 4\gamma^2 I^2 A^2 L_0^2 \eta + 4\gamma^2 I^2 B^2 L_1^2 \eta \|\nabla f(\bar{\mathbf{x}}_t)\|^2 + \frac{50 A L_0 \eta^2 \sigma^2}{N} + \frac{B L_1 \gamma^2 \|\nabla f(\bar{\mathbf{x}}_t)\|}{2}\right] \\
&\overset{(b)}{\leq} \frac{1}{N}\sum_{t=0}^{T-1}\mathbb{E}\sum_{i\in J(t)}[P_1 + P_2\|\nabla f(\bar{\mathbf{x}}_t)\|] \\
&\quad + \frac{1}{N}\sum_{t=0}^{T-1}\mathbb{E}\sum_{i\in \bar{J}(t)}\left[-\frac{\eta c_{\min}}{4}\|\nabla f(\bar{\mathbf{x}}_t)\|^2 + 4\gamma^2 I^2 A^2 L_0^2 \eta + \frac{50 A L_0 \eta^2 \sigma^2}{N} + \frac{B L_1 \gamma^2 \|\nabla f(\bar{\mathbf{x}}_t)\|}{2}\right],
\end{aligned} \tag{19}$$

where (a) holds due to Lemma 3, and

$$P_1 = -\frac{3\gamma^2}{5\eta} + \frac{7\gamma}{5}\sigma + \frac{14\gamma^2 I A L_0}{5} + A L_0 \gamma^2 + \frac{50 A L_0 \eta^2 \sigma^2}{N},$$
$$P_2 = -\frac{2\gamma}{5} + \frac{14\gamma^2 I B L_1}{5} + \frac{B L_1 \gamma^2}{2},$$

(b) is derived by computing

$$4\gamma^2 I^2 B^2 L_1^2 \eta \leq \frac{4N^2\epsilon^4 I^2 B^2 c_{\min}^2 L_1^2 \eta}{28^2 \sigma^2 A^2 L_0^2} \leq \frac{4B^2 c_{\min}^2 L_1^2 \epsilon^4 \eta}{28^2 \sigma^2 A^2 L_0^2} \underbrace{\frac{28^2 A^2 L_0^2}{25 B^2 L_1^2 \epsilon^2}}_{\text{bound of } N^2} \underbrace{\frac{\sigma^2}{c_{\min} N^2 \epsilon^2}}_{\text{bound of } I^2} \leq \frac{\eta}{4} c_{\min} \tag{20}$$

with $N \leq \min\{\frac{1}{\epsilon}, \frac{14AL_0}{5BL_1\epsilon}\}$, $\gamma \leq c_{\min}\frac{N\epsilon}{28\sigma}\min\{\frac{\epsilon}{AL_0}, \frac{1}{BL_1}\}$, and $I \leq \sqrt{\frac{1}{c_{\min}}}\frac{\sigma}{N\epsilon}$.

Now we give the upper bound of P_1 and P_2.

From the choice of $N \leq \min\{\frac{1}{\epsilon}, \frac{14AL_0}{5BL_1\epsilon}\}$, $\gamma \leq c_{\min}\frac{N\epsilon}{28\sigma}\min\{\frac{\epsilon}{AL_0}, \frac{1}{BL_1}\}$, $I \leq \sqrt{\frac{1}{c_{\min}}}\frac{\sigma}{N\epsilon}$ and the fixed ratio $\frac{\gamma}{\eta} = 5\sigma$, and noting that $\sigma \geq 1$, we have

$$\begin{aligned}
P_1 &\leq \left(-\frac{3}{5}\cdot 5\sigma + \frac{7}{5}\sigma + \frac{\epsilon}{10} + \frac{\epsilon}{28}\right)\gamma + \frac{50 A L_0 \eta^2 \sigma^2}{N} \leq -\frac{3}{10}\gamma\sigma + \frac{50 A L_0 \eta^2 \sigma^2}{N}, \\
P_2 &\leq \left(-\frac{2}{5} + \frac{1}{10} + \frac{\epsilon}{10}\right)\gamma \leq -\frac{1}{10}\gamma.
\end{aligned} \tag{21}$$

Plugging (21) back to (19), we obtain

$$-\Delta \leq -(f(\bar{\mathbf{x}}_0) - f_*) \leq \mathbb{E} f(\bar{\mathbf{x}}_T) - f(\bar{\mathbf{x}}_0) \leq \mathbb{E}\left[\frac{1}{N}\sum_{t=0}^{T-1}\sum_{i\in J(t)} U(\bar{\mathbf{x}}_t) + \frac{1}{N}\sum_{t=0}^{T-1}\sum_{i\in \bar{J}(t)} V(\bar{\mathbf{x}}_t)\right],$$

where

$$
\begin{aligned}
U(\bar{\mathbf{x}}_t) &= -\frac{1}{10}\gamma\|\nabla f(\bar{\mathbf{x}}_t)\| - \frac{3}{10}\gamma\sigma + \frac{50AL_0\eta^2\sigma^2}{N}, \\
V(\bar{\mathbf{x}}_t) &= -\frac{\eta c_{\min}}{4}\|\nabla f(\bar{\mathbf{x}}_t)\|^2 + 4\gamma^2 I^2 A^2 L_0^2\eta + \frac{50AL_0\eta^2\sigma^2}{N} + \frac{BL_1\gamma^2\|\nabla f(\bar{\mathbf{x}}_t)\|}{2} \\
&\overset{(a)}{\leq} -\frac{\eta c_{\min}\epsilon}{2}\|\nabla f(\bar{\mathbf{x}}_t)\| + \frac{BL_1\gamma^2\|\nabla f(\bar{\mathbf{x}}_t)\|}{2} + \frac{\eta c_{\min}\epsilon^2}{4} + 4\gamma^2 I^2 A^2 L_0^2\eta + 50AL_0\frac{\eta^2}{N}\sigma^2 \\
&\overset{(b)}{\leq} -\frac{\eta c_{\min}\epsilon}{4}\|\nabla f(\bar{\mathbf{x}}_t)\| + \frac{\eta c_{\min}\epsilon^2}{4} + 4\gamma^2 I^2 A^2 L_0^2\eta + 50AL_0\frac{\eta^2}{N}\sigma^2.
\end{aligned}
$$

Inequality (a) follows by using the standard inequality $x^2 \geq 2\epsilon x - \epsilon^2$ and (b) is true because

$$
-\frac{\eta c_{\min}\epsilon}{2} + \frac{BL_1\gamma^2}{2} \leq \frac{-\eta c_{\min}\epsilon}{4}. \tag{22}
$$

To check (22), note that $\gamma \leq c_{\min}\frac{N\epsilon^2}{28AL_0\sigma}$, we compute

$$
BL_1\gamma^2 \leq BL_1 \cdot 5\eta\sigma\frac{c_{\min}N\epsilon^2}{28AL_0\sigma} = \eta\frac{5Bc_{\min}L_1N\epsilon^2}{28AL_0} \leq \frac{\eta c_{\min}\epsilon}{2}, \tag{23}
$$

where the last inequality holds because we assume $N \leq \frac{14AL_0}{5BL_1\epsilon}$.

It's clear that $U(\mathbf{x}) \leq V(\mathbf{x})$. Then we obtain

$$
-\Delta \leq -(f(\bar{\mathbf{x}}_0) - f_*) \leq \mathbb{E}\left[\sum_{t=0}^{T-1} V(\bar{\mathbf{x}}_t)\right] \leq \sum_{t=0}^{T-1}\left[-\frac{\eta c_{\min}\epsilon}{4}\mathbb{E}\|\nabla f(\bar{\mathbf{x}}_t)\| + \frac{\eta c_{\min}\epsilon^2}{4} + 4\gamma^2 I^2 A^2 L_0^2\eta + 50AL_0\frac{\eta^2}{N}\sigma^2\right].
$$

Then we rearrange the above inequality, take $T \geq \frac{1}{c_{\min}^2}\frac{560AL_0\Delta\sigma^2}{N\epsilon^4}$ and $I \leq \sqrt{\frac{1}{c_{\min}}}\frac{\sigma}{N\epsilon}$. Then we can guarantee that

$$
\frac{4\Delta}{\epsilon\eta c_{\min}T} \leq \epsilon, \frac{4AL_0\eta\sigma^2}{c_{\min}N\epsilon} \leq \frac{4\epsilon}{28\times 5} = \frac{\epsilon}{35}, \frac{16\gamma^2 I^2 A^2 L_0^2}{c_{\min}\epsilon} \leq \epsilon,
$$

and hence we have

$$
\frac{1}{T}\sum_{t=1}^{T}\mathbb{E}\|\nabla f(\bar{\mathbf{x}}_t)\| \leq \frac{4\Delta}{\epsilon\eta c_{\min}T} + \epsilon + \frac{200AL_0\eta\sigma^2}{c_{\min}N\epsilon} + \frac{16\gamma^2 I^2 A^2 L_0^2}{c_{\min}\epsilon} \leq 9\epsilon.
$$

The theorem is proved. □

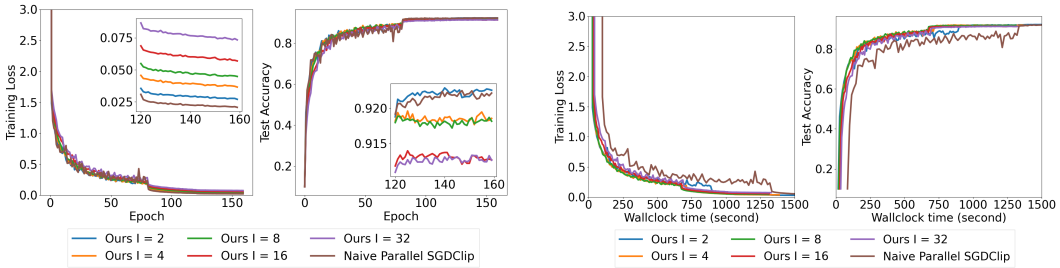

(a) Over epoch

(b) Over wall clock time

Figure 7: Training loss and test accuracy v.s. (Left) epoch and (right) wall clock time on training a 32 layer Resnet to do image classification on CIFAR10.

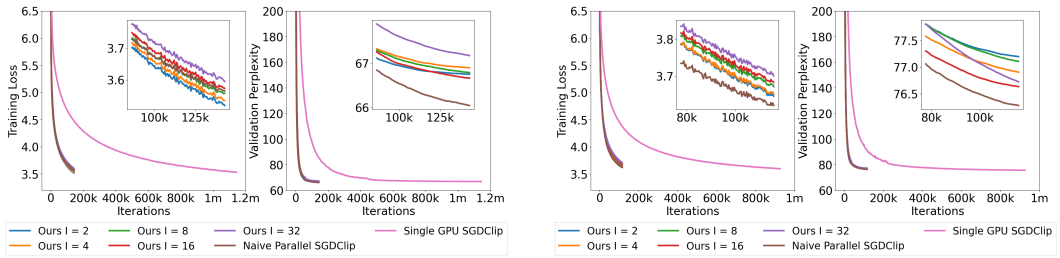

(a) Penn Treebank

(b) Wikitext-2

Figure 8: Performance v.s. # of iterations each GPU runs on training AWD-LSTMs to do language modeling on Penn Treebank (left) and Wikitext-2 (right) showing the parallel speedup.

D More Experiment Results

D.1 CIFAR-10 classification with ResNet-32

Apart from the 56 layer Resnet used in Section 5, we also trained the 32 layer Resnet on CIFAR-10. Here, we used a smaller minibatch size of 16 per GPU. We also used SGD with clipping for the baseline algorithm with a stagewise decaying learning rate schedule, We set the initial learning rate $\eta = 0.1$ and the clipping parameter $\gamma = 1.0$. We decrease both η and γ by a factor of 10 at epoch 80 and 120. These parameter settings follow that of [50].

Results reported in Figure 7 again show that our algorithm can not only match the baseline in both training loss and test accuracy epoch-wise but is way better in terms of wall-clock time for moderate values of I.

D.2 Parallel Speedup on NLP Tasks

In Section 5.2 we have shown the parallel speedup effects of our algorithm on training a Resnet model on the CIFAR10 dataset. Here we present the same phenomena but on training AWD-LSTMs on doing language modeling on Penn Treebank and Wikitext-2 in Figure 8.

Again, note that in the distributed setting, one iteration means running one step of Algorithm 1 on all machines; while in the single machine setting, one iteration means running one step of SGD with clipping. For Penn Treebank, we use minibatch size 3 on every GPU in the distributed setting to run Algorithm 1, while we also use 3 minibatch size on the single GPU to run SGD with clipping. For Wikitext-2, the corresponding minibatch size is 10.

Figure 8 again clearly shows that even with $I > 1$, our algorithm still enjoys parallel speedup, since our algorithm requires less number of iterations to converge to the same targets (e.g., training loss, validation perplexity). This observation is consistent with our iteration complexity results in Theorem 1.

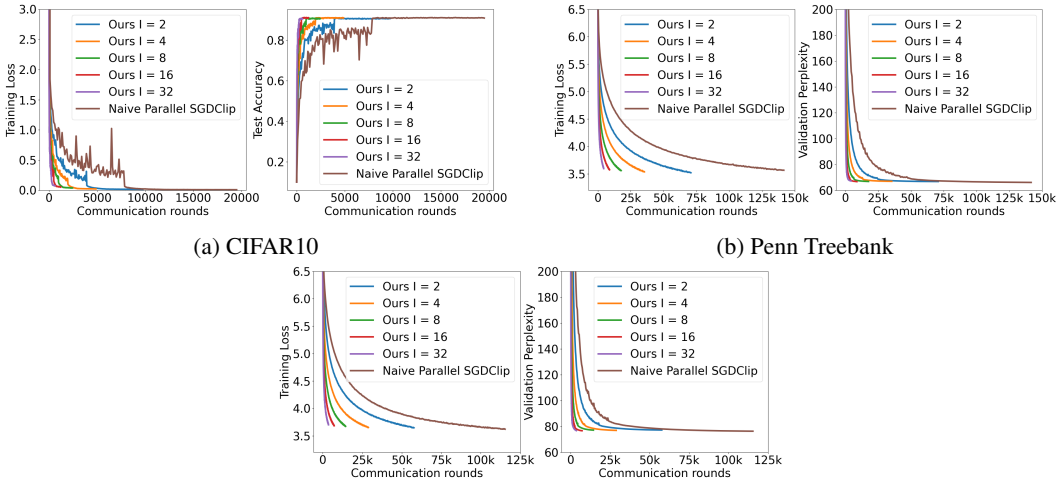

(a) CIFAR10

(b) Penn Treebank

(c) Wikitext-2

Figure 9: Performance v.s. # of communication rounds each GPU conducts on training (a) Resnet-56 on CIFAR10 (b) AWD-LSTM on Penn Treebank (c) AWD-LSTM on Wikitext-2.

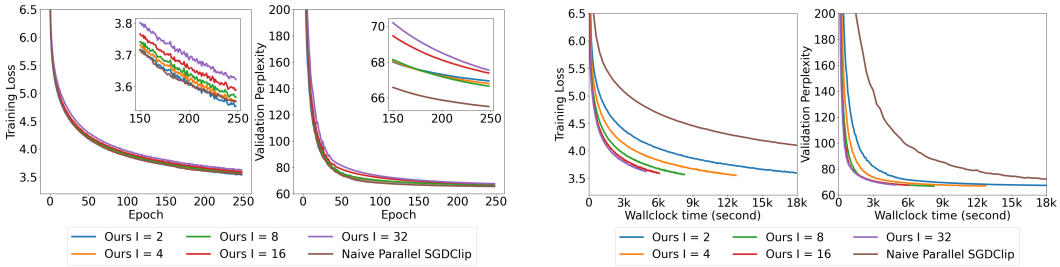

(a) Over epoch

(b) Over wall clock time

Figure 10: Train an AWD-LSTM to do language modeling on Penn Treebank where only a subset of nodes participate in each communication.

D.3 Performance vs. Communication Rounds

The reader might be interested in how the training and testing performance changes w.r.t. the number of communications each machine does for both the Naive Parallel SGDClip and our CELGC with different I. Thus, we show such results in Figure 9. The results are very close to that w.r.t. the wall-clock time which is as expected.

D.4 Partial Participation

In the previous experiments, when communication between nodes occurs, all nodes send their model and/or gradients for averaging and update accordingly. Yet, in practice, it might be that only a (different) subset of nodes participates in communication each time. Therefore, we conduct an experiment in this setting. Specifically, we take the Penn Treebank dataset and train the AWD-LSTM of the same structure as in Section 5.1 to do language modeling. However, when the algorithm requires communication across nodes, we randomly select 6 out of the total 8 nodes to communicate and average the model and/or gradient and update those 6 nodes only; the rest 2 nodes will be left untouched. Considering that this setting introduces a big difference compared with the setting we adopted in Section 5.1, we finely tuned the initial learning rate for both the baseline and our algorithm and picked the one that gives the smallest training loss.

The results are reported in Figure 10. We can see that, though the partial participation setting slightly deteriorates the performance for both the baseline and our algorithm as compared with Figure 2a, our algorithm is still able to closely match the baseline for both the training loss and the validation

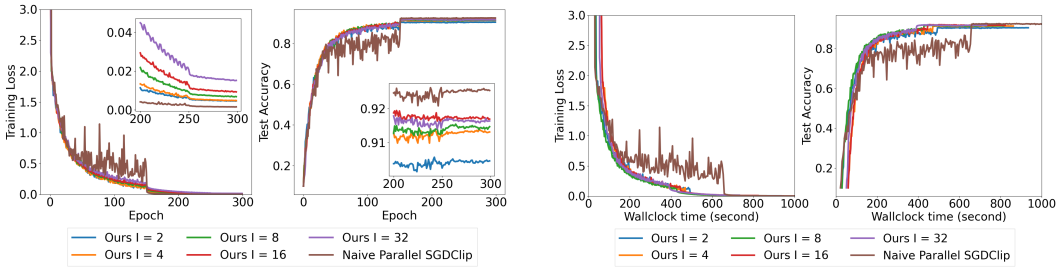

(a) Over epoch

(b) Over wall clock time

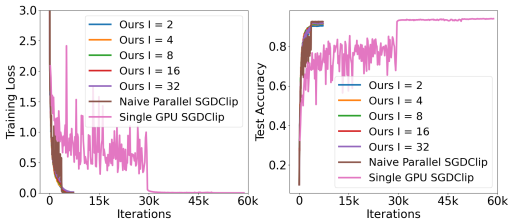

(c) Over # of iterations each GPU runs

Figure 11: Algorithm 1 with different I: Training loss and test accuracy v.s. (a) epoch, (b) wall clock time, and (c) # of iterations each GPU runs on training a 56 layer Resnet to do image classification on CIFAR10 with local mini-batch size 256 on each node.

perplexity epoch-wise, but also note that our algorithm greatly saves wall-clock time. This indicates that our algorithm is robust in the partial participation setting.

Finally we want to remark that the our main proof of Theorem 1 can be easily extended to the partial client participation case since the source of randomness of partical participation can be decoupled with the other source of randomness in the algorithm.

D.5 Large Mini-batch

The distributed learning paradigm is especially desirable with training using large mini-batches. To this end, we trained a Resnet-56 model on CIFAR10 with batch-size 256 on each node which sums up to a batch size of 2048 globally. Compared with the experiment in Section 5.1, considering the large batch-size, we trained for 300 epochs instead of 200, decrease the learning rate by a factor of 10 at epoch 150 and 250, and finely tuned the initial learning rate for each variant and picked the one that gives the smallest training loss. Results are shown in Figure 11. Similar to the small-batch case reported in Figure 1, our algorithm with skipped communication is able to match the naive parallel SGDClip in terms of epochs but greatly speeds up wall-clock-wise. Also, Figure 11c again verifies the parallel speed-up property of our algorithm.

D.6 Compare with Naive Parallel SGDClip when each Method Uses Same Amount of Data between each Communication

To provide another perspective to compare our algorithm with Naive Parallel SGDClip, we design another experiment following the spirit of [44]. We compared our algorithm for different communication intervals I with Naive Parallel SGDClip with I times larger mini-batch sizes and communicating at each iteration. The goal is to ensure that between two neighboring communication rounds, each method use the same number of oracle calls. The results are reported in Figure 12, from which we can clearly see that our method enjoys a substantial lead and the advantage becomes more and more significant as we use larger I values. This observation is inline with the common issue of large batch training in deep neural networks.

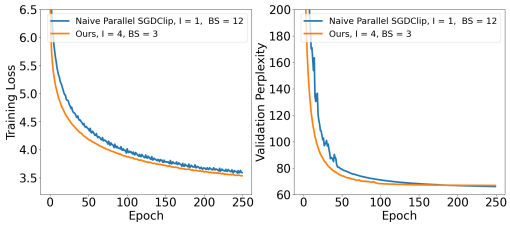

(a) Ours $I = 4$ vs. Baseline BS 12

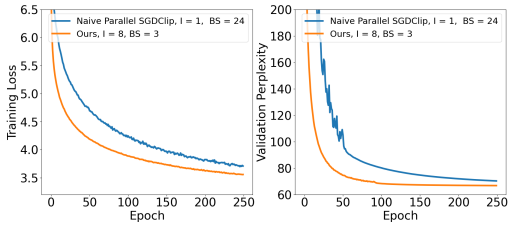

(b) Ours $I = 8$ vs. Baseline BS 24

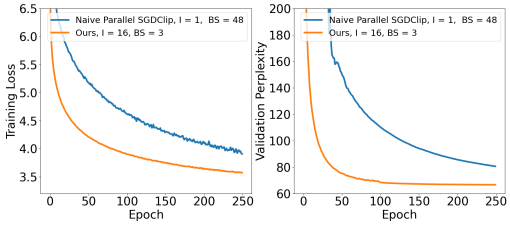

(c) Ours $I = 16$ vs. Baseline BS 48

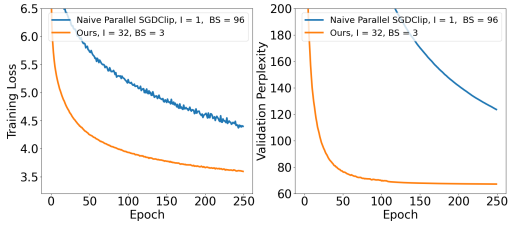

(d) Ours $I = 32$ vs. Baseline BS 96

Figure 12: Training loss and validation perplexity on training an AWD-LSTM to do language modeling on Penn Treebank: our algorithm with different communication interval value I vs. Naive Parallel SGDClip with I times larger batch size and communicating at each iteration (We use "BS" to denote batchsize.)

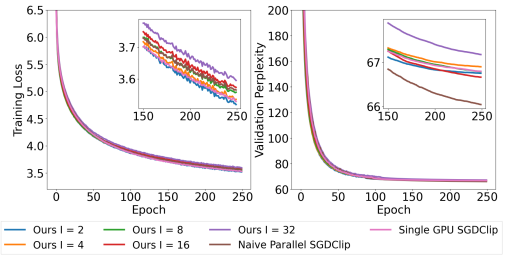

Figure 13: Performance vs. epoch on training an AWD-LSTM to do language modeling on Penn Treebank showing linear speedup.

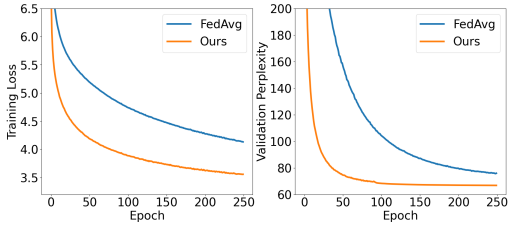

Figure 14: Train an AWD-LSTM by FedAvg / ours, both with communication interval $I = 8$, to do language modeling on Penn Treebank.

D.7 Linear Speedup

In Figure 13, we compared our algorithm's performance with Single GPU SGDClip over number of epochs. Clearly, all variants of ours can match the latter epoch-wise. Note that the mini-batch size in each GPU is the same for all, and ours use 8 GPU; thus, for each GPU, the number of iterations in one epoch of ours is exactly $1/8$ of that of Single GPU SGDClip. Hence, we have empirically verified the linear speedup property.

D.8 Comparison with FedAvg which has No Clipping

Figure 5 shows that clipping is very frequent, especially in the language modeling task on Penn Treebank. In our view, frequent clipping indicates the importance of clipping since otherwise, the training may encounter exploding gradient problems and even diverge. Indeed, without clipping, FedAvg behaves much worse, as shown in Figure 14.

D.9 Heterogeneous Setting

In the previous experiments, all machines can access the whole dataset. Yet, in practice, each machine might only access a subset of the whole dataset and the data might not be evenly distributed across machines. Therefore, we conduct an experiment on this heterogeneous setting. Specifically, we take the Penn Treebank training set which is a text file and divide it into 8 non-overlapping consecutive

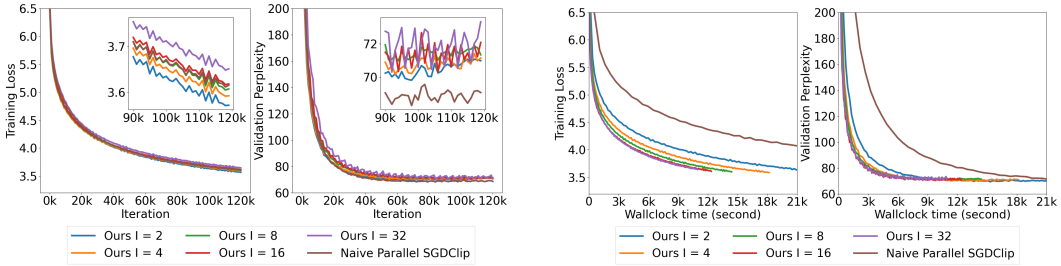

(a) Over epoch

(b) Over Wall clock time

Figure 15: Training an AWD-LSTM to do language modeling on Penn Treebank in a heterogeneous setting where each node accesses only a different subset of the whole dataset.

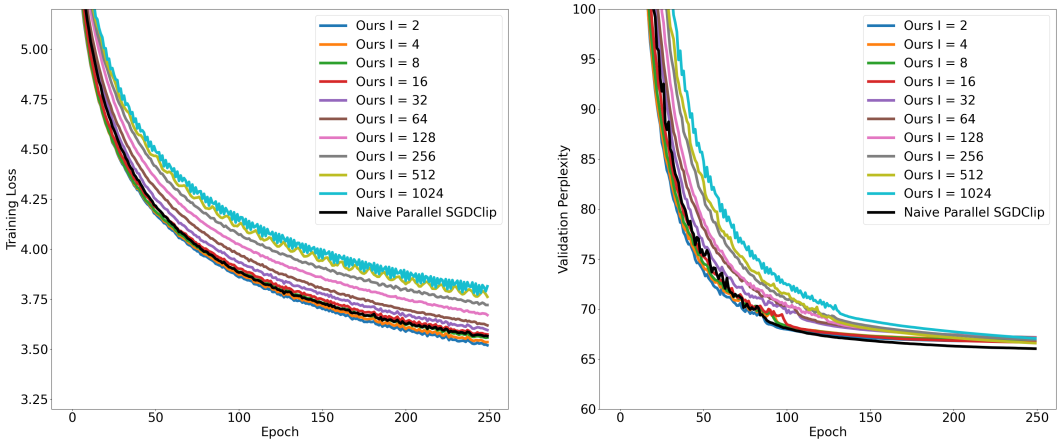

Figure 16: Performance vs. epoch on training an AWD-LSTM to do language modeling on Penn Treebank with large I.

parts which contain $\{10.64\%, 11.17\%, 11.70\%, 12.23\%, 12.77\%, 13.30\%, 13.83\%, 14.36\%\}$ of the whole text file respectively. We then train the AWD-LSTM of the same structure as in Section 5.1 to do language modeling. Considering that the heterogeneous setting introduces a big difference compared with the setting we adopted in Section 5.1, we finely tuned the initial learning rate for both the baseline and our algorithm and picked the one that gives the smallest training loss.

The results are reported in Figure 15. Note that, as the size of training data in each machine is different, we draw the training and testing performance curves over the number of iterations each machine runs instead of epochs. This means that, if the x-axis value is 1000, then each GPU runs 1000 iterations. We can see that, though the unbalancing and heterogeneity of the training data deteriorates the performance for both the baseline and our algorithm as compared with Figure 2a, our algorithm is still able to surpass the baseline in training losses though it falls slightly behind in testing; meanwhile, our algorithm obtains significant speedup in terms of wall-clock time. This suggests that our algorithm is robust to the heterogeneous setting.

D.10 Performance of Large Communication Intervals

To investigate how our algorithm behaves when I, the communication interval, becomes very large, we conducted an experiment of training the AWD-LSTM model to do language modelling on Penn Treebank with exponentially increasing I. The results are shown in Figure 16. As can be seen, the training performance deteriorates quickly as I increases.

D.11 Our Algorithm Coupled with Momentum

Given that momentum is commonly employed when using SGD to train neural networks, we conduct an experiment on comparing CELGC with momentum of different I with the naive parallel SGDClip

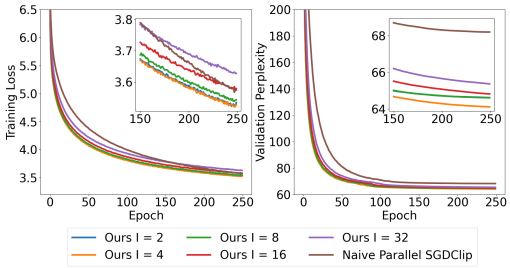

Figure 17: Performance vs. epoch on training an AWD-LSTM to do language modeling on Penn Treebank when all optimizers use momentum.

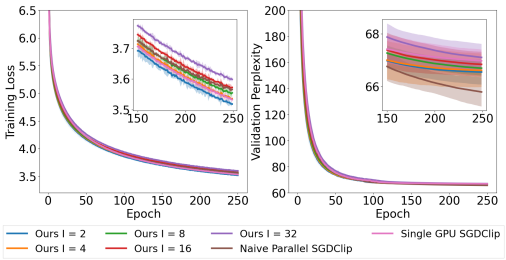

Figure 18: Performance vs. epoch on training an AWD-LSTM to do language modeling on Penn Treebank. The shading of each curve represents the 95% confidence interval computed across 3 independent runs from different random seeds.

Table 2: Average final training loss and validation perplexity achieved by each method when traning an AWD-LSTM to do language modeling on Penn Treebank (Figure 18). The $\pm$ shows 95% confidence intervals of the mean value over three runs starting from different random seeds.

Methods	Training loss	Validation perplexity
Our CELGC $I = 2$	3.5184 ± 0.0018	66.5486 ± 0.4746
Our CELGC $I = 4$	3.5357 ± 0.0025	66.6117 ± 0.6340
Our CELGC $I = 8$	3.5548 ± 0.0116	66.6968 ± 0.2771
Our CELGC $I = 16$	3.5724 ± 0.0016	66.8406 ± 0.4755
Our CELGC $I = 32$	3.5989 ± 0.0092	67.1035 ± 0.5124
Naive Parallel SGDClip	3.5658 ± 0.0055	65.7935 ± 0.5534
Single GPU SGDClip	3.5328 ± 0.0104	66.9757 ± 0.4259

with momentum. Specifically, we train an AWD-LSTM to do language modeling on Penn Treebank, and use a momentum parameter $\beta = 0.9$ and a clipping threshold $\gamma = 2.5$ following [50]. The results are shown in Figure 17, from which we can see that our algorithm can still match the naive parallel SGDClip with momentum very well. This indicates that our algorithm couples well with the momentum technique.

D.12 Multiple Runs Showing Confidence Interval

To show that our results is stable over random seeds, we train an AWD-LSTM to do language modeling on Penn Treebank over three independent runs from different random seeds. The results are shown in Figure 18 and Table 2. It can be seen that our results are stable.

D.13 Final Results in Tables

To facilitate easier comparison, we summarize results of above experiments in following tables.

E The Distribution of Stochastic Gradient Values

In this section, we empirically verify Assumption 1 (iv) in the training of an AWD-LSTM on the Penn Treebank dataset to do language modeling. We investigate the setting of distributed training using 8 GPUs with $I = 4$. For details on experiment setting and hyperparameter choices, please refer to Section 5.

At the end of each epoch we investigate, we average the local models across all machines. We then fix this model and run it over the whole training set to compute all mini-batch stochastic gradients. Finally, we randomly select a set of coordinate pairs and draw their respective 1-D value distributions and 2-D joint distribution. The results are shown in Figure 19 and 20. We can clearly see that the distributions exhibit symmetry around the mean and monotonically decreasing probability density as the ℓ_2 distance to the mean increases. These results support the use of Assumption 1 (iv).

Table 3: Final results on training Resnets to do image classification on CIFAR-10.

(a) 56 layer Resnet with local mini-batch size 64 (Figure 1, 4& 9a)

Methods	Training Loss	Test Accuracy
Ours I = 2	0.0146	0.9076
Ours I = 4	0.0216	0.9109
Ours I = 8	0.0372	0.9068
Ours I = 16	0.0544	0.9104
Ours I = 32	0.0745	0.9070
Naive Parallel SGDClip	0.0087	0.9114
Single GPU SGDClip	0.0020	0.9410

(b) 56 layer Resnet with local mini-batch size 256 (Figure 11)

Methods	Training Loss	Test Accuracy
Ours I = 2	0.0046	0.9046
Ours I = 4	0.0048	0.9131
Ours I = 8	0.0068	0.9147
Ours I = 16	0.0092	0.9169
Ours I = 32	0.0152	0.9163
Naive Parallel SGDClip	0.0015	0.9253
Single GPU SGDClip	0.0012	0.9402

(c) 32 layer Resnet with local mini-batch size 16 (Figure 7)

Methods	Training Loss	Test Accuracy
Ours I = 2	0.0269	0.9225
Ours I = 4	0.0365	0.9185
Ours I = 8	0.0448	0.9181
Ours I = 16	0.0569	0.9127
Ours I = 32	0.0733	0.9127
Naive Parallel SGDClip	0.0207	0.9221

Table 4: Final results on training an AWD-LSTM to do language modeling on Wikitext-2 (Figure 3, 8b& 9c).

Methods	Training Loss	Validation Perplexity
Ours I = 2	3.6461	77.1938
Ours I = 4	3.6512	76.9033
Ours I = 8	3.6716	77.1042
Ours I = 16	3.6833	76.6340
Ours I = 32	3.7006	76.7249
Naive Parallel SGDClip	3.6207	76.2834
Single GPU SGDClip	3.5960	75.6326

Table 5: Final results on training an AWD-LSTM to do language modeling on Penn Treebank.

(a) Homogeneous setting (Figure 2, 8a, 9b, 13,& 16)

Methods	Training Loss	Validation Perplexity
Ours I = 2	3.5191	66.7519
Ours I = 4	3.5352	66.8982
Ours I = 8	3.5576	66.7906
Ours I = 16	3.5731	66.6629
Ours I = 32	3.5951	67.1752
Ours I = 64	3.6186	67.1609
Ours I = 128	3.6702	67.1126
Ours I = 256	3.7205	66.9107
Ours I = 512	3.7615	66.5976
Ours I = 1024	3.8139	67.0686
Naive Parallel SGDClip	3.5648	66.0435
Single GPU SGDClip	3.5290	66.7948

(b) Partial participation setting (Figure 10)

Methods	Training Loss	Validation Perplexity
Ours I = 2	3.5384	66.9437
Ours I = 4	3.5528	66.7992
Ours I = 8	3.5671	66.6489
Ours I = 16	3.5896	67.3863
Ours I = 32	3.6229	67.5515
Naive Parallel SGDClip	3.5535	65.5083

(c) Heterogeneous setting (Figure 15)

Methods	Training Loss	Validation Perplexity
Ours I = 2	3.5640	70.7216
Ours I = 4	3.5848	70.8548
Ours I = 8	3.5989	71.2799
Ours I = 16	3.6092	70.6850
Ours I = 32	3.6428	70.4912
Naive Parallel SGDClip	3.6021	68.5727

(d) Our Algorithm Coupled with momentum (Figure 17)

Methods	Training Loss	Validation Perplexity
Ours I = 2	3.5348	64.6153
Ours I = 4	3.5278	64.1062
Ours I = 8	3.5435	64.6068
Ours I = 16	3.5788	64.8165
Ours I = 32	3.6276	65.3660
Naive Parallel SGDClip	3.5747	68.2008

Table 6: Final results on training Resnet-50 to do image classification on ImageNet (figure 6).

Methods	Training Loss	Test Accuracy
Goyal et al., 2018 [12]	0.7792	0.7610
Naive Parallel SGDClip	0.7795	0.7626
CELGC I=4	0.7795	0.7607

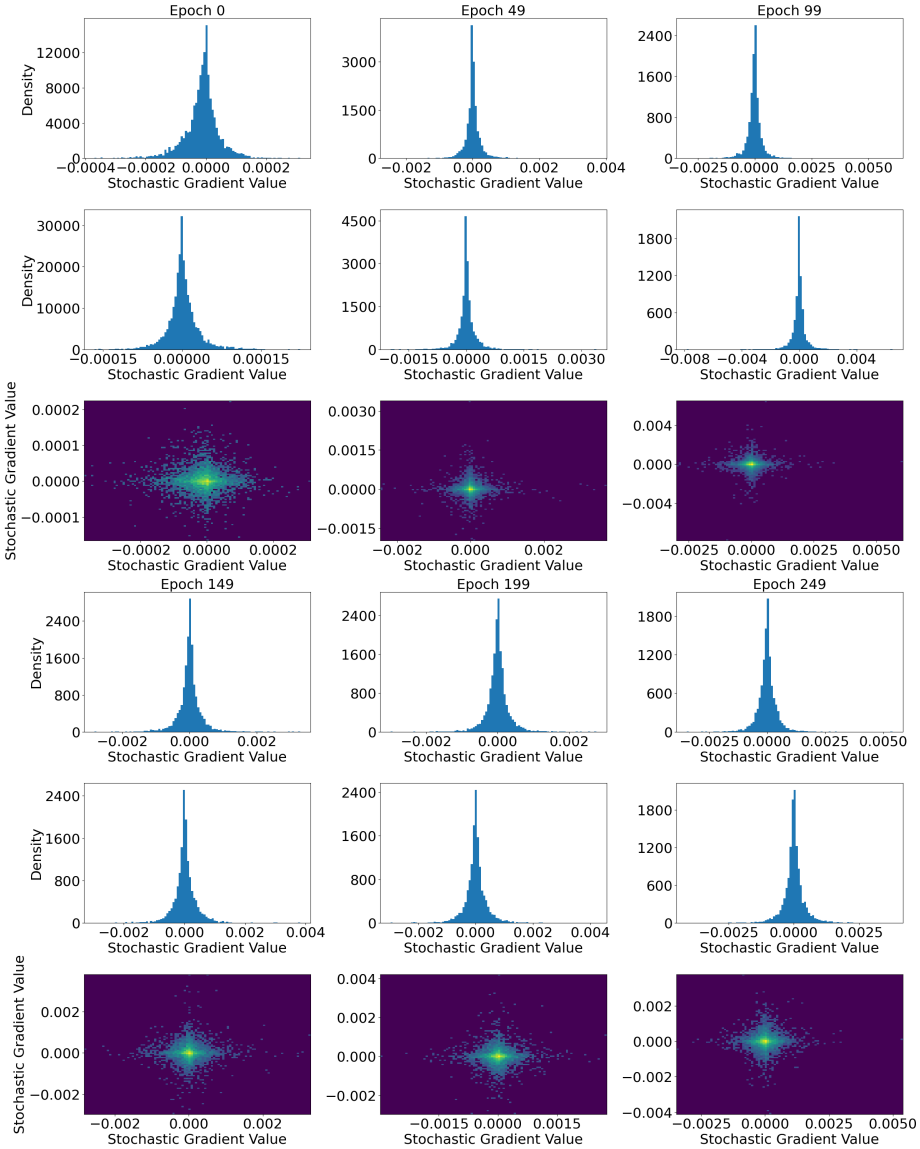

Figure 19: During training an AWD-LSTM in the Penn Treebank dataset, we randomly selected two coordinates and drew the distribution of the stochastic gradient values at these coordinates over the whole training set. The 1st and 4th rows belong to one coordinate, the 2nd and 5th rows belong to another coordinate, and the 3rd and 6th rows depict their joint distribution. We can clearly see that the stochastic gradients observe symmetric distributions with monotonically decreasing probability density along the distance to the mean.

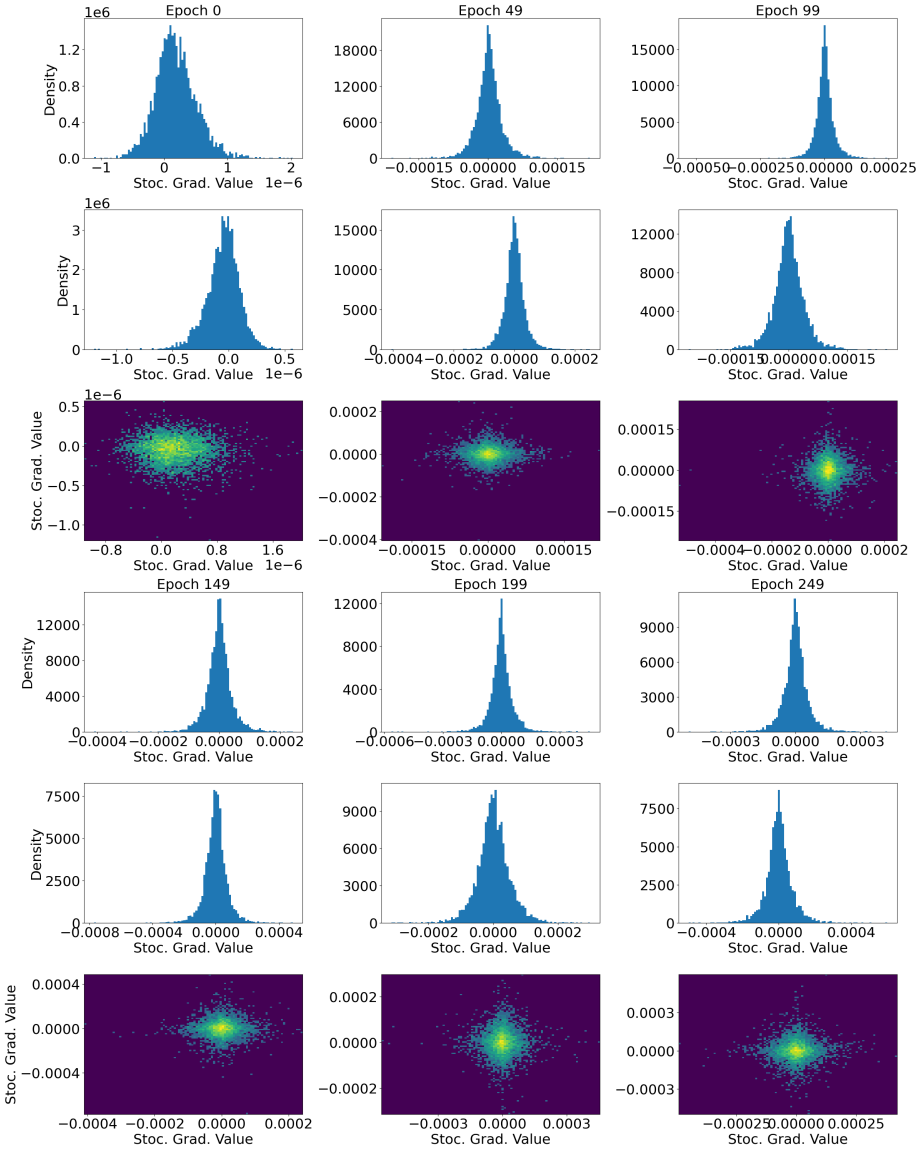

Figure 20: During training an AWD-LSTM in the Penn Treebank dataset, we randomly selected two coordinates and drew the distribution of the stochastic gradient values at these coordinates over the whole training set. The 1st and 4th rows belong to one coordinate, the 2nd and 5th rows belong to another coordinate, and the 3rd and 6th rows depict their joint distribution. We can clearly see that the stochastic gradients observe symmetric distributions with monotonically decreasing probability density along the distance to the mean.